


RESEARCH ARTICLE OPEN ACCESS

Development of a Recombinant Outer Membrane Vesicles (OMVs)-Based Vaccine Against *Helicobacter pylori* Infection in Mice

Qiong Liu^{1,2,3} | Biaoxian Li^{1,2,3,4} | Jinrong Ma^{1,3,4} | Xiao Lei¹ | Junpeng Ma^{1,3,4} | Yanyan Da^{1,3,4} | Zhiyong Zhou^{1,3,4} | Jiaqi Tao^{1,3,4} | Xinyi Ren^{1,3,4} | Ting Zeng^{1,3,4} | Zhiting Xie^{1,3,4} | Haiyan Lin^{1,3,4} | Zihui Jin^{1,3,4} | Yi Wan^{1,3,4} | Liang Zhang^{1,3,4} | Donglin Lai^{1,3,4} | Yaping Guo^{1,3,4} | Jing Li^{1,3,4} | Yinpan Shang² | Lu Shen² | Ziwei Tao² | Tian Gong^{1,3,4} | Chengsheng Zhang^{1,3,4} 

¹Center for Molecular Diagnosis and Precision Medicine, The First Affiliated Hospital, Jiangxi Medical College, Nanchang University, Nanchang, China |

²Department of Medical Microbiology, School of Basic Medical Sciences, Jiangxi Medical College, Nanchang University, Nanchang, China | ³Jiangxi Provincial Center for Advanced Diagnostic Technology and Precision Medicine, The First Affiliated Hospital, Jiangxi Medical College, Nanchang University, Nanchang, China | ⁴Department of Medical Genetics, The First Affiliated Hospital, Jiangxi Medical College, Nanchang University, Nanchang, China

Correspondence: Tian Gong (ndyfy09649@ncu.edu.cn) | Chengsheng Zhang (ndyfy09564@ncu.edu.cn)

Received: 5 January 2025 | **Revised:** 8 April 2025 | **Accepted:** 12 April 2025

Funding: Funding was received from National Natural Science Foundation of China 82203032 and 32260193 (Qiong Liu), Project for high and talent of Science and Technology Innovation in Jiangxi “double thousand plan” jxsq2023301110 (Qiong Liu), the start-up fund from the First Affiliated Hospital of Nanchang University 500021010 (Chengsheng Zhang) and the fund from School of Basic Medical Sciences, Nanchang University (Qiong Liu).

Keywords: *H. pylori* | LPS | OMVs | recombinant vaccine

ABSTRACT

The current vaccine development for *Helicobacter pylori* (*H. pylori*) still faces challenges of weak immune responses stimulated by existing antigens and a lack of safe adjuvants. The modification of the lipopolysaccharide (LPS) structure by *H. pylori* is an important mechanism involved in its immune escape. In this study, we developed a novel recombinant vaccine candidate against *H. pylori* infection by knocking down the key genes (*lpxE*, *lpxF* and *futB*) of LPS modification and employing the bacterial outer membrane vesicles (OMVs) as a vector for delivering UreB, VacA and CagA antigens, and then evaluated its safety and immune protective efficacy in vitro and in vivo mouse model. We measured the antibody and cytokine productions, detected the subtypes of immune cells, and examined the histopathological changes in mice from the control and various experimental groups. We revealed that this OMV-based recombinant vaccine candidate could induce specific humoral immune responses and a Th1/Th2/Th17 mixed immune response, with Th17 being predominant, and markedly protect the mice from *H. pylori* infection. Our findings suggest that the OMVs with the genetically engineered LPS may function as a vector for delivering recombinant antigens and safe adjuvants for the development of novel vaccine candidates against *H. pylori* infection.

Qiong Liu and Biaoxian Li contributed equally to this work.

This is an open access article under the terms of the [Creative Commons Attribution-NonCommercial-NoDerivs](https://creativecommons.org/licenses/by-nc-nd/4.0/) License, which permits use and distribution in any medium, provided the original work is properly cited, the use is non-commercial and no modifications or adaptations are made.

© 2025 The Author(s). *Journal of Extracellular Vesicles* published by Wiley Periodicals LLC on behalf of International Society for Extracellular Vesicles.

1 | Introduction

Helicobacter pylori (*H. pylori*) is a gram-negative bacterium that colonises exclusively at the gastric mucosa and is associated with the pathogenesis of gastrointestinal diseases such as gastritis, gastric ulcers and malignancy in the stomach. *H. pylori* infection rate is extremely high, affecting nearly half of the population of the world (Wang et al. 2024). Antibiotics are currently the most common and effective treatment for *H. pylori* infection (Liou et al. 2024). However, antimicrobial resistance in different parts of the world has become a major challenge, which has driven the development of vaccine candidates, including whole-cell inactivated vaccines and DNA vaccines (Li et al. 2024). Despite the efforts, the production of an effective vaccine against *H. pylori* infection is still facing a number of challenges, including the immune escape phenomenon of *H. pylori* (Dos Santos Viana et al. 2021). Therefore, it is urgently needed to explore novel vaccine design strategies to develop an effective vaccine against *H. pylori* infection.

Vaccines based on components of spontaneously produced outer membrane vesicles (OMVs) of bacteria and their use as delivery vehicles have been of increasing interest to researchers. OMVs, as products of the bacterial outer membrane, contain not only lipopolysaccharide (LPS), the main component of the outer membrane, but also a number of other immunogenic molecules, which make them good candidates for vaccine development (Tan et al. 2018). OMV-based vaccines have been developed and tested for their efficacy against many bacterial diseases (Kaparakis-Liaskos and Ferrero 2015), such as the meningococcal group B OMV vaccine (Seib et al. 2015). In addition, Keenan and colleagues previously reported that *H. pylori* could produce OMVs, but there has been no report on the potential application of OMVs as a vaccine against *H. pylori* infection (Keenan et al. 1997). Our previous studies have also demonstrated that wild-type *H. pylori* OMVs are immunogenic and could be a good vaccine candidate (Song et al. 2020), and their safety has been confirmed in mouse experiments (Liu et al. 2019). At the same time, the pathogen-associated molecular patterns (PAMPs) and other various components encapsulated in the OMVs allow them to be used as an adjuvant in vaccine development (Tan et al. 2018). Thus, OMVs can serve as an effective fusion of a self-adjuvant vaccine type and antigen delivery vector. Moreover, the immune escape phenomenon caused by *H. pylori* LPS provides us with new ideas for further improving the use of OMVs as an efficient vaccine and antigen delivery vector.

The immune escape phenomenon of *H. pylori* is closely related to its LPS structure. For instance, its lipid A structure is tetra-acyl lipid A, which lacks 4' phosphate in the presence of *lpxE*, while the 1' phosphate group is acylated in the presence of *lpxF* (Cullen et al. 2011). Compared to the lipid A in other Gram-negative bacteria, it cannot be well bound by Toll-like receptor 4 (TLR4) to elicit an immune response, and this helps *H. pylori* to evade clearance of the host immune response during colonisation (Cullen et al. 2011; Maldonado et al. 2016). Further, the O-polysaccharide antigen (O antigen) structure in LPS has a molecular mimicry phenomenon. The polymeric N-acetyl- β -lactosamine (LacNAc) chain could decorate with multiple lateral α -L-fucose residues forming internal Lewis X (Le^x) determinants with terminal Le^x or Lewis Y (Le^y) determinants, and Le^x and Le^y

are modified by the action of fucosyltransferases such as FutA and FutB to form a structure similar to the Lewis (Le) antigen in serum thus allowing *H. pylori* to undergo immune evasion even during long-term infection, or to cause host autoimmune disease, resulting in *H. pylori* infection not being easily cleared (Maldonado et al. 2016). Therefore, it is necessary to eliminate the effect of immune evasion caused by LPS so that the OMVs can induce an efficient immune response. The key genes are *futA* and *futB*, and studies have shown that the *futA* mutation does not affect Le^y but strongly decreases Le^x , while the *futB* mutation greatly reduces Le^y expression but increases polymeric Le^x (Moran 2008). Moreover, the antibody corresponding to the Le^x antigen can promote the anti-*H. pylori* infection (Rudnicka et al. 2001). At the same time, Le^x antigen can induce a higher level of cellular immune response in C57BL/6 mice compared with Le^y antigen (Suresh et al. 2000), which indicates that reducing the synthesis of Le^y antigen and increasing polymeric Le^x antigen can potentially improve the immune protective efficacy of LPS-modified OMVs and *futB* gene was therefore selected as a potential target gene to enhance vaccine potential.

In addition, the self-adjuvant effect of OMVs also endows them with the potential to serve as efficient delivery vector for vaccines. Therefore, major antigen proteins can be expressed on the surface of OMVs to enhance their protective efficacy as vaccines. Urease B (UreB), vacuolating cytotoxin A (VacA) and cytotoxin-associated antigen (CagA) are three crucial antigenic proteins in *H. pylori* that induce host immune responses (Liu et al. 2011). Consequently, exploring innovative antigen delivery strategies for *H. pylori* vaccines represents a critical challenge. In our study, we aimed to construct a six-fatty acid chain lipid A structure in *H. pylori* by knocking out *lpxF* and *lpxE* genes, thereby restoring the ability to be recognised by TLR4 and exhibiting adjuvant activity. Additionally, we blocked the synthesis of Le antigen structure by knocking down *futB* gene. To develop a highly protective *H. pylori* OMVs vaccine, we utilised the haemoglobin protease (Hbp) autotransporter system to express the primary *H. pylori* antigenic proteins (UreB, VacA and CagA) on the surface of OMVs. We then analysed the immune protection and anti-*H. pylori* infection efficacy in mice. Through this approach, we anticipate selecting an optimal antigen combination to develop a vaccine candidate, ultimately paving the way for further advancements in the prevention and treatment of *H. pylori* infection.

2 | Materials and Methods

2.1 | Bacteria, Plasmids, Media and Growth Conditions

The strains of *H. pylori* and plasmids used in this study are shown in Table S1. *H. pylori* 7.13, derived from clinical strain B128 and *H. pylori* J99, were gifts from Dr. Yong Xie at the First Affiliated Hospital of Nanchang University in China. Suspensions of *H. pylori* 7.13 used for the immune challenge experiment were prepared from fresh exponential phase cultures to maintain a high level of viable cells. All strains were cultured in Campylobacter Agar bases (Difco Labs, Detroit, MI, USA) containing 10% sheep blood (Thermo Fisher Scientific, North Shore City, New Zealand) and *H. pylori* selective supplement (Dent, 10 μ g/mL vancomycin, 5 μ g/mL trimethoprim lactate, 5 μ g/mL cefsulodin sodium and

5 µg/mL amphotericin B) in a microaerobic environment (5% O₂, 10% CO₂ and 85% N₂) at 37°C.

2.2 | Construction of *H. pylori* LPS Modified Mutations and Related Plasmids

Mutant strains were constructed using the suicide plasmid method. The upstream and downstream homologous arms of *lpxE* were amplified by PCR, ligated to the kanamycin resistance gene marker (Kan⁺) and inserted into the pRE112 suicide plasmid backbone. The transformed plasmid was transferred into the J99 strain by electroporation to construct the Δ *lpxE* mutant, and the transformants were screened with LB agar plates containing the appropriate antibiotics. The same strategy was used to construct PHQ013 and PHQ014 plasmids using chloramphenicol resistance (Cm⁺) and ampicillin resistance gene markers (Amp⁺) to construct Δ *lpxF* and Δ *futB* mutants, respectively. The triple knockout strains Δ *lpxE* Δ *lpxF* Δ *futB* were constructed using PHQ012, PHQ013 and PHQ014 with the same strategy.

Daleke-Schermerhorn and colleagues demonstrated the capability of the Hbp autotransporter platform to incorporate multiple antigenic proteins into a vector plasmid and express them on the surface of OMVs (Daleke-Schermerhorn et al. 2014). Based on this finding, we employed the genomic DNA of *Salmonella* Typhimurium χ 3761 as a template, utilising Hbp-F and Hbp-R primers to concurrently amplify gene fragments of the Hbp autotransporter platform and the linearised plasmid pQS1, which was based on pYA3337 and inserted a spectinomycin resistance gene to transfer the plasmid into *H. pylori* for construction selection. The primers used are listed in Table S2. We cloned the Hbp autotransporter platform expression cassette into the pYA3337 vector using a Gibson assembly kit and transformed it into *Escherichia coli* (*E. coli*) strain TOP10 for amplification, resulting in the pYA3337-Hbp plasmid, named pQS2. Subsequently, we utilised the Hbp autotransporter platform to clone the antigenic protein gene sequences into the Hbp expression cassette within the recombinant plasmid pQS2.

To achieve this, we first amplified the UreB gene sequence from the *H. pylori* genome using corresponding primers and cloned it into the prepared recombinant plasmid pQS2 using a one-step cloning technique with a Gibson assembly kit. The resultant plasmid was transformed into *E. coli* TOP10 cells to generate the recombinant pQS2-UreB plasmid, named pQS0007. Similarly, we amplified other antigenic protein gene sequences from the *H. pylori* genome using specific primers and obtained the recombinant plasmids pQS0008 (VacA) and pQS0009 (CagA).

Further, we amplified the VacA antigenic protein gene and the vector from the *H. pylori* genome and the vector plasmid pQS0007 (UreB), respectively, using corresponding primers. After one-step cloning of the amplified product using a Gibson assembly kit, the product was transformed into *E. coli* TOP10 cells to generate the recombinant plasmid pQS0004 (UreB-VacA). The CagA gene sequence was incorporated using the same method to yield the recombinant plasmid pQS0005 (UreB-CagA). We also introduced the CagA gene sequence into the recombinant plasmid pQS0008 (VacA) to create the recombinant plasmid pQS0006 (VacA-CagA). Additionally, we used the recombinant plasmid pQS0004

(UreB-VacA) as the vector, amplified it using the upstream and downstream primers of plasmid pQS0009 (CagA), and cloned the amplified CagA gene sequence and the vector into *E. coli* TOP10 cells to obtain the recombinant plasmid pQS0003 (UreB-VacA-CagA). Finally, the recombinant plasmids were transformed into competent *H. pylori* cells to express the antigenic proteins UreB, VacA and CagA.

2.3 | Purification and Identification of OMVs

H. pylori OMVs were isolated through ultracentrifugation, as previously described (Liu et al. 2016; Liu et al. 2018). Briefly, 500 mL cultures of wild-type and mutant strains of *H. pylori* in exponential phase were centrifuged at 4500 × g for 1 h at 4°C to precipitate the bacteria. The supernatant was then filtered twice through a 0.45 µm Steritop bottle-top filter unit (Millipore, Billerica, MA, USA). The filtered supernatant containing OMVs was centrifuged at 20,000 × g for 2 h at 4°C, and the resultant pellet was washed with Dulbecco's phosphate-buffered saline (DPBS) buffer (Mediatech, Manassas, VA, USA). The pelleted OMV samples were resuspended in DPBS buffer containing OptiPrep Density Gradient Medium (Sigma) and centrifuged for 24 h at 100,000 × g at 4°C in a density gradient ranging from 40% to 20%. The vesicle fractions were pooled, gently washed three times with DPBS, and then resuspended in 1 mL of DPBS for storage at −20°C. The yields of OMVs were determined by measuring protein concentrations using a bicinchoninic acid (BCA) assay kit (Thermo Fisher, Rockford, IL, USA), following the manufacturer's instructions. The morphology of the OMVs was examined by transmission electron microscopy (TEM) at 120 kV (Tecnai Spirit). The expression of different proteins in the OMVs was detected by immunoblotting using rabbit serum antibodies against UreB, VacA or CagA (UreB, Cat. Orb359898, Biorbyt; VacA, Cat. Orb51658, Biorbyt; CagA, Cat. Orb23539, Biorbyt). The particle size distribution and concentration of OMVs were determined by nanoparticle tracking analysis (NanoSight NS300, Malvern Instruments, UK), as previously described (White et al. 2018; Chen et al. 2020). The average of triplicate video statistics was calculated for each sample. Additionally, the number of OMVs per millilitre was normalised to the colony-forming units (CFUs) per millilitre for each strain to assess the number of OMVs per CFU.

2.4 | Purification and Identification of Lipid A and O Antigens

Cultures (500 mL) were incubated at 37°C under microaerobic conditions for 36–40 h until A600 was 1.0. Cells were collected by centrifugation at 6000 rpm for 15 min, washed once with phosphate-buffered saline, and then suspended in 20 mL of phosphate-buffered saline to release lipid A from the cells, which were placed on thin-layer chromatography plates (TLC) and separated using the solvents chloroform, pyridine, 88% formic acid and water in a 50:50:16:5 ratio by volume. The TLC plates were exposed to the phosphorus imager screen overnight, and the product formation was detected and analysed using a phosphate molecular imager equipped with Quantity One software. ESI-MS analysis was performed using a 0.1% formic acid, 230 min acetonitrile gradient, and further observed by SDS-PAGE after

silver staining. The phenol was placed in a constant temperature water bath at 65°C for preheating. After the strain was incubated for 72 h, 2 mL of 1xPBS was added to the culture dish, and the surface of the dish was repeatedly blown to dislodge the bacteria, and the rinsed PBS was dispensed into sterile endotoxin-free centrifuge tubes. The above steps were repeated four times. Then centrifuge at 4°C 12,000 rpm for 20 min, pour off the supernatant, add 675 µL of ultrapure water and 675 µL of pre-warmed phenol to each tube, and repeatedly blow the white precipitate with a gun to dissolve it. After shaking for 1 min, place it in a constant temperature water bath at 65°C for 10 min, then centrifuge at 12,000 rpm for 10 min at 4°C. Transfer the upper aqueous phase to a new sterile endotoxin-free centrifuge tube, add an equal volume of ether as the amount transferred, shake to mix, centrifuge at 12,000 rpm for 3 min at 4°C, repeat four times, and pour off the upper layer of ether. Open the lid of the centrifuge tube and place it in a fume hood overnight. Add 0.2 mg RNaseA, 0.2 mg DNaseI to each centrifuge tube, thermostatic water bath at 37°C for 30 min, then add 0.08 mg Proteinase K respectively, thermostatic water bath at 60°C for 1 h, then thermostatic water bath at 100°C for 3 min. The LPS was analysed to identify the modified O antigen by western blotting using mouse anti-Lewis A (Le^a) (Cat. sc-59469), anti-Lewis B (Le^b) (Cat. sc-59470), anti-Le^x (Cat. sc-59471), anti-Le^y (Cat. sc-59469) (Santa Cruz, USA) and anti-H type 1 (Cat. 667551) (BioLegend, USA).

2.5 | TLR Signalling Assay

Human epithelial kidney (HEK) 293 cells stably co-transfected with mouse or human TLR4 and myeloid differentiation factor 2 (TLR4-MD2) receptors (noted as m/hTLR4-MD2) were purchased from InvivoGen. All cell lines stably expressed secretory embryonic alkaline phosphatase (SEAP) under the control of nuclear NF-κB and activator protein 1 (AP-1)-induced promoters. Thus, stimulation of m/hTLR4-MD2 would result in an amount of SEAP in the extracellular supernatant proportional to the level of NF-κB induction. The cells were cultured in standard Dulbecco's modified Eagle's medium (DMEM) containing 10% heat-inactivated foetal bovine serum (Gibco), 4.5 g/L glucose, 2 mM L-glutamine, 50 U/mL penicillin, 50 µg/mL streptomycin and 1xHEK-Blue Selection (InvivoGen), and maintained at 37°C in a 5% saturated CO₂ atmosphere.

Cells were inoculated in 96-well plates at 2 × 10⁴ cells/well, and highly purified LPS was added in triplicate at concentrations of 0, 10, 100, 1000 and 10,000 µg/mL, respectively, and the average value was taken. LPS of *E. coli* (TLR4 agonist) (Sigma-Aldrich) was used as a positive control. After 20–24 h of incubation, 20 µL of supernatant is transferred to a new 96-well plate and then incubated 1–2 times at 37°C with 180 µL of QUANTI-Blue. The activity of SEAP was measured by reading the optical density at 655 nm with a Synergy Mx multi-mode microplate reader (BioTek) to evaluate the binding ability of modified LPS to TLR4 in HEK-m/hTLR4 cells (Cullen et al. 2011).

2.6 | Activation of Dendritic Cells (DC)

Primary DC cells were obtained from mice and cultured for 5–8 d in RPMI-1640 complete medium (containing 10% FCS) with 500

U/mL IL-4 and 800 U/mL GM-CSF (both from Schering-Plough) for 5–8 d (Geijtenbeek et al. 2000). To analyse maturation, 180,000 DCs were co-incubated with *H. pylori* OMVs for 12 h, washed and cultured for 20 h, and analysed for maturation markers (CD80, CD86, CD83 and HLA-DR) by flow cytometry (Geijtenbeek et al. 2003).

2.7 | Evaluation of OMV Cytotoxicity at the Cellular Level

The cytotoxicity of OMVs on RAW264.7 macrophages was assessed using 24-well plates seeded with 5 × 10⁵ cells per well and exposed to varying concentrations of OMVs (ranging from 3.125 to 100 µg/mL) (Liu et al. 2016). After a 24-h incubation period, the supernatants were collected from each well, and cytotoxicity was quantified using a Multitox-Fluor multiplex cytotoxicity assay kit (Promega, Madison, WI, USA), following the manufacturer's instructions. All experiments were conducted in triplicate, and the collected data will be analysed subsequently.

2.8 | Animal Experiments

All animal experiments were conducted in compliance with the guidelines of the Animal Welfare Act and related regulations of The First Affiliated Hospital of Nanchang University (Nanchang, China, Approval No. CDYFY-IACUC-202305QR024). All animal work protocols were approved by the animal welfare committee of The First Affiliated Hospital of Nanchang University. The principles stated in the Guide for the Care and Use of Laboratory Animals were followed. All efforts were made to minimise animal suffering during the experiments.

Specific pathogen-free (SPF) female C57BL/6 mice (6 weeks old, 16–22 g) were purchased from the Laboratory Animal Science Centre of Nanchang University. After acclimatisation to the new environment for 1 week, the mice were randomly divided into various groups. Each group contained 6–12 mice and received the first vaccine administration by gavage (0 day). The selected immunogens and dosages administered to each group are described in Tables S3 and S4. Blood samples were collected 1 day prior to 4 and 8 weeks following the first immunisation through orbital sinus puncture. Subsequently, the soluble fractions of serum were obtained by centrifugation. Booster immunisations were performed at Week 4 with corresponding antigens by intragastric vaccination. Some of the mice were executed at Week 8, and approximately 500 mg of gastric tissue was collected and stored in 500 µL of 2% saponin (Sigma)-PBS solution overnight at 4°C to prepare gastric extract for mucosal secretory IgA detection following the method described previously (Kimoto et al. 2019). Splenocytes and mesenteric lymph node (MLN) cells were collected and assayed for cytokine production. Ten weeks after the first immunisation, all remaining mice were challenged with 10⁹ CFU of virulent *H. pylori* 7.13 (Asim et al. 2015) in 20 µL PBS containing 0.01% gelatin (BSG buffer) via the oral route and monitored until Week 16. Finally, all mice were sacrificed, and their gastric tissues were harvested for urease tests and bacterial load determination. All animal experiments were performed twice, and the data were gathered for analysis.

2.9 | Biodistribution Kinetic Analysis of OMVs

In order to examine the biological distribution of OMVs in mice after immunisation, we administered OMVs or Cy7-labelled OMVs to mice by oral administration and observed the changes of OMVs in various tissues over time through in vivo imaging and immunofluorescence staining following the protocol described previously (Jang et al. 2015). In brief, the mice were treated by oral administration of OMVs or Cy7-labelled OMVs (15 µg of total protein) or PBS. The biodistribution of OMVs was analysed by near-infrared (NIR) imaging at 0, 3, 6, 12 and 24 h post treatment. Cy7 fluorescence in the whole body of mice was observed by IVIS spectrum (Caliper Life Sciences). At each time point, mice were sacrificed and Cy7 fluorescence was observed in various tissues including liver, stomach, spleen, kidney, heart and small intestines. Radiant efficiency was measured using Living Image 3.1 software. After 1, 3 and 7 days, gastric tissue was sectioned for immunofluorescence assay using the anti-wt OMV primary antibody and the corresponding HRP-conjugated secondary antibody, then the nuclei were counterstained with DAPI and observed with a FLUOVIEW FV1000 confocal laser scanning microscope (Olympus).

2.10 | ELISA

Antibody levels in mouse blood samples and stomach tissues were measured using ELISA as previously described (Liu et al. 2016). The inactivated whole cell antigen and outer membrane proteins (OMPs) as coating antigens were prepared based on the previous study (Song et al. 2020). Inactivated whole cell antigens, OMPs and LPS from wild type *H. pylori* J99 and mutants were suspended in 100 µL sodium carbonate buffer (pH = 9.6), and 1 µg of suspension per well was added to 96-well plates (Nalge Nunc Inc., Naperville, IL, USA) for antigen encapsulation and incubated overnight at 4°C. Purified mouse immunoglobulin standards (IgG, IgG₁, IgG_{2c} or IgA; BD Biosciences, MA, USA) were added to each well in triplicate and diluted 2-fold (0.5 µg/µL). The plates were then washed three times with PBS containing 0.1% Tween 20 (PBST) and closed with 2% BSA solution for 2 h at room temperature. 100 µL of each sample was added to the respective wells in triplicate at different dilutions and incubated at room temperature for 1 h. After washing the plates three times with PBST and biotinylated goat anti-mouse antibodies IgG, IgG₁, IgG_{2c} and IgA (Southern Biotech Inc., Birmingham, AL, USA) were added to each well, respectively. The alkaline phosphatase coupling compound (Southern Biotechnology) was added, and the substrate nitrobenzene phosphatase (Sigma-Aldrich) was added to diethanolamine buffer (pH = 9.8) to develop the colour in each well. Determination of the absorbance at 405 nm using a fully automated ELISA microplate reader (model EL311SX; BioTek, Winooski, VT, USA). Final Ig isotype concentrations were calculated separately for each antibody isotype sample using a standard curve.

2.11 | Urease Test

Gastric antrum tissue homogenates were prepared from tissue strips obtained from each mouse. Approximately 500 mg of gastric tissues were collected and placed in 0.5 mL of 0.8% NaCl solution for detection of urease activity (Nedrud and Blanchard

2001). Homogenates from mice injected with either PBS or OMVs devoid of *H. pylori* antigenic proteins served as negative controls. Initially, 100 µL of tissue homogenate was mixed with 3 mL of urea broth (composed of 1 mg/mL glucose, 1 mg/mL peptone, 2 mg/mL KH₂PO₄, 5 mg/mL NaCl and 1% urea), which contained the phenol red indicator. The mixture was then incubated at 37°C for 4 h. Subsequently, gastric urease activity was spectrophotometrically assayed at an optical density of 550 nm.

2.12 | Determination of Bacterial Loading

Mice were orally dosed with *H. pylori* 7.13 for the challenge protection assay, and gastric tissues were collected after 6 weeks for bacterial load determination. First, isolated tissues were washed with pre-chilled PBS and then transferred to pre-weighed tubes containing 5 mL of brain heart infusion (BHI) medium (Difco). Next, gastric tissues were reweighed to an accuracy of 0.0001 g, homogenised with a sterile homogeniser and serially inoculated onto Campylobacter agar matrix (Difco) plates containing 10% sheep blood at dilutions of 1:10, 1:100 and 1:1000. The plates were then incubated at 37°C under microaerobic conditions for 6–7 days. Colonies were identified as *H. pylori* by urease reaction, oxidase reaction and wet morphological analysis. Urease specimens were removed from the stomach of each mouse and immersed in 0.5 mL of 0.8% NaCl solution to make a tissue homogenate for determination of urease activity as described above (Nedrud and Blanchard 2001). Tissue homogenates containing PBS were used as a negative control.

2.13 | Detection of Cytokines in Mouse MLN Cells and Splenocytes

Mouse MLN cells and splenocytes were harvested 4 weeks after booster immunisations, followed by stimulation with 6 µg/mL OMPs isolated from *H. pylori* 7.13 strain, and OMPs or OMVs isolated from *H. pylori* J99 strain for 24 h as previously described (Song et al. 2020). Then, the supernatants of those cells were collected, and cytokine levels were quantified by ELISA. Monoclonal anti-interferon-γ (anti-IFN-γ), anti-IL-4, anti-IL-6, anti-IL-12 (P40), anti-IL-13 and anti-IL-17 antibodies (BD Biosciences, Mountain View, CA, USA) were coated onto 96-well plates. Then, samples were blocked with PBS containing 1% bovine serum albumin, added to triplicate wells and incubated overnight at 4°C. Then, the plates were washed and incubated with biotin-labelled anti-IFN-γ, anti-IL-12 (P40), anti-IL-4, anti-IL-13, anti-IL-17 and anti-IL-6 antibodies (BD Biosciences, Billerica, MA, USA). Finally, horseradish peroxidase-labelled anti-biotin antibodies (Vector Laboratories, Burlingame, CA, USA) were added to each well along with 3,3',5,5'-tetramethylbenzidine (TMB; Moss Inc., Pasadena, CA, USA) to enhance the reaction, which was terminated with 0.5 M hydrochloric acid (HCl). Standard curves were generated based on the expression levels of mouse recombinant IFN-γ, IL-4, IL-6, IL-12 (P40), IL-13 and IL-17.

2.14 | Histopathology

Two weeks post-challenge with *H. pylori*, mouse stomachs were harvested for histopathological analysis, conducted according to a previously reported method (Ghasemi et al. 2022). Briefly,

stomach tissues were fixed in 10% neutral buffered formalin for a minimum of 24 h, followed by processing, paraffin embedding and sectioning at 5 μ m. The sections were stained with haematoxylin and eosin. The pathologist was blinded to the experimental groups and treatments. Both glandular and squamous portions of the stomach were histologically examined and evaluated, with scoring based on criteria including mucosal inflammation and type (0–6 intensity), submucosal inflammation and type (0–6 intensity), mucosal ulceration (0–6 intensity) and hyperkeratosis of the squamous stomach (0–6 intensity).

2.15 | Flow Cytometry

Splenocytes were suspended in 2 mL of Roswell Park Memorial Institute medium supplemented with 100 IU/mL penicillin-streptomycin and 10% foetal bovine serum, and plated in 12-well plates. The cells were then stimulated with 2 μ g of CD28 and 40 μ g of OMVs derived from different mutations for 24 h at 37°C in 5% CO₂. In the final 6 h of incubation, protein transport inhibitors brefeldin A (2 μ L/mL; BD Biosciences, NJ, USA) and monensin (1.4 μ L/mL; BD Biosciences) were added to the cells. Following centrifugation, the supernatant was discarded, and 2 μ L of Fc receptor blocker (BioLegend) was added to the cell suspension. Subsequently, 5 μ L of premixed True-Stain Monocyte Blocker (Biolegend) and 2 μ L of CD4 (Biolegend) were added to the cell suspension and incubated in the dark at room temperature for 25 min. The cells were then washed with PBS and incubated in 1 mL of diluted Zombie Aqua solution (Biolegend) for 10 min, followed by centrifugation. The cells were subsequently fixed, permeabilised and washed according to the instructions provided with the Fixation/Permeabilisation Kit (BD). After each centrifugation step, the obtained cell clusters were added to a mixture containing 10 mL of Brilliant Stain Buffer Plus (BD), 5 mL of True-Stain Monocyte Blocker (Biolegend), 2 mL of anti-CD3 (Biolegend), 2 mL of anti-CD154 (Biolegend), 2 mL of anti-IL-17A (Biolegend) and 2 mL of anti-IFN- γ (Biolegend), and thoroughly mixed. The cells were incubated in the dark at room temperature for 30 min with BD Perm/Wash Buffer and PBS, before being resuspended in 0.2 mL of PBS. Finally, the number of various cell types was determined using a flow cytometer.

2.16 | Statistical Analysis

All ELISA experiments were performed in triplicate. The significance of differences in the average values between the experimental and control groups was assessed using one-way or two-way analysis of variance (ANOVA) tests and followed by Tukey's post hoc test. All data are expressed as mean \pm standard deviation (SD) and analysed statistically using GraphPad Prism software version five (GraphPad Software Inc., San Diego, CA, USA).

3 | Results

3.1 | Identification of *H. pylori* OMVs With Modified LPS Structure

To verify the modifications of lipid A in the mutant *H. pylori* strains, lipid A was purified, separated by TLC, and detected

by phospholipid imaging (Figure 1A). Different mutant strains showed different mobility than wild-type J99, indicating a successful modification of lipid A structure. To further determine the structural modifications of lipid A, lipid A of all strains was analysed by ESI-MS (Figure 1B). As expected, wild-type J99 had a predominant peak at m/z 1546.9, representing a tetraacylated structure (lack of 4' phosphate while the 1' phosphate group is acylated). The $\Delta lpxE$ mutant is predicted to retain the unacylated 1' phosphate group and the $\Delta lpxF$ mutant to retain the 4' phosphate, and their mass spectra peaks show a left and right shift, respectively, compared to the wild type. The peak of the mass spectrum of the double $\Delta lpxE \Delta lpxF$ mutants was significantly smaller than that of the $\Delta lpxF$ mutant, with a slight increase compared to that of the wild-type and $\Delta lpxE$ mutant. These results indicated the target structure of lipid A. Further examination of the lipid A structure after silver staining revealed that the double $\Delta lpxE \Delta lpxF$ mutants and $\Delta lpxE \Delta lpxF \Delta futB$ mutants showed obviously different structure from the wild-type J99, also confirming the successful modification of lipid A (Figure 1C) (Cullen et al. 2011; Tran et al. 2006; Schmidinger et al. 2022). The O antigen in *H. pylori* LPS has a Le structure that has been identified as having a molecular mimicry phenomenon, which mediates immune escape of pathogenic bacteria (Maldonado et al. 2016; Tang et al. 2023). We knocked down *futB* to eliminate this structure, allowing the OMVs to better stimulate the host immune responses. The SDS-PAGE results showed that the modification of lipid A caused changes in the band size of LPS. The migration of the lipid A in the $\Delta lpxE \Delta lpxF$ mutant strain is slower than that in the wild-type J99, while $\Delta futB$ does not show a significant effect on the band size of LPS (Figure 1D). Thus, immunoblotting is needed to confirm this. To verify the modified O antigen, western blotting was performed to analyse LPS from the wild type versus the mutant type (Figure 1E–G). LPS from the $\Delta lpxE \Delta lpxF \Delta futB$ mutants and $\Delta futB$ mutant were found to be unable to react with Le^x and Le^y antigen sera, indicating that the modified O antigen no longer had a Le type 2 structure. The Le expression of the wild-type strain 7.13 was known to be H type 1, and using it as a positive control, it was found that the mutant did not react with the H type 1 antigen serum, indicating successful disruption of the Le antigen expression. In addition, neither the modified LPS of *H. pylori* J99 strain nor the LPS of wild-type strain could react to Le^a and Le^b antibodies (Data not shown). These results demonstrate that the modification of the O antigen has achieved the desired goal.

TEM and Nanoparticle tracking analysis were used to determine the particle size of the OMVs and the concentrated fraction during density gradient purification (Théry et al. 2018). The results showed that most of the OMVs produced by the mutant and parental strains were between 80 and 89 nm in diameter and that the OMVs released from the mutant strains did not differ significantly compared to the wild-type strain, indicating that the knockout did not affect the particle size and yield of the OMVs (Figures 1H and S1). To determine whether the OMVs secreted by the modified *H. pylori* were toxic to cells, OMVs derived from the mutant and wild-type strains were purified and incubated with RAW264.7 cells at different concentrations for 24 h. The cell lysis set was used as a quality control. Compared with the wild-type strain, OMVs from the mutant strains showed some cytotoxicity at concentrations above 25 μ g/mL, but the cytotoxic effect was not obvious at lower concentrations (Figure 1I).

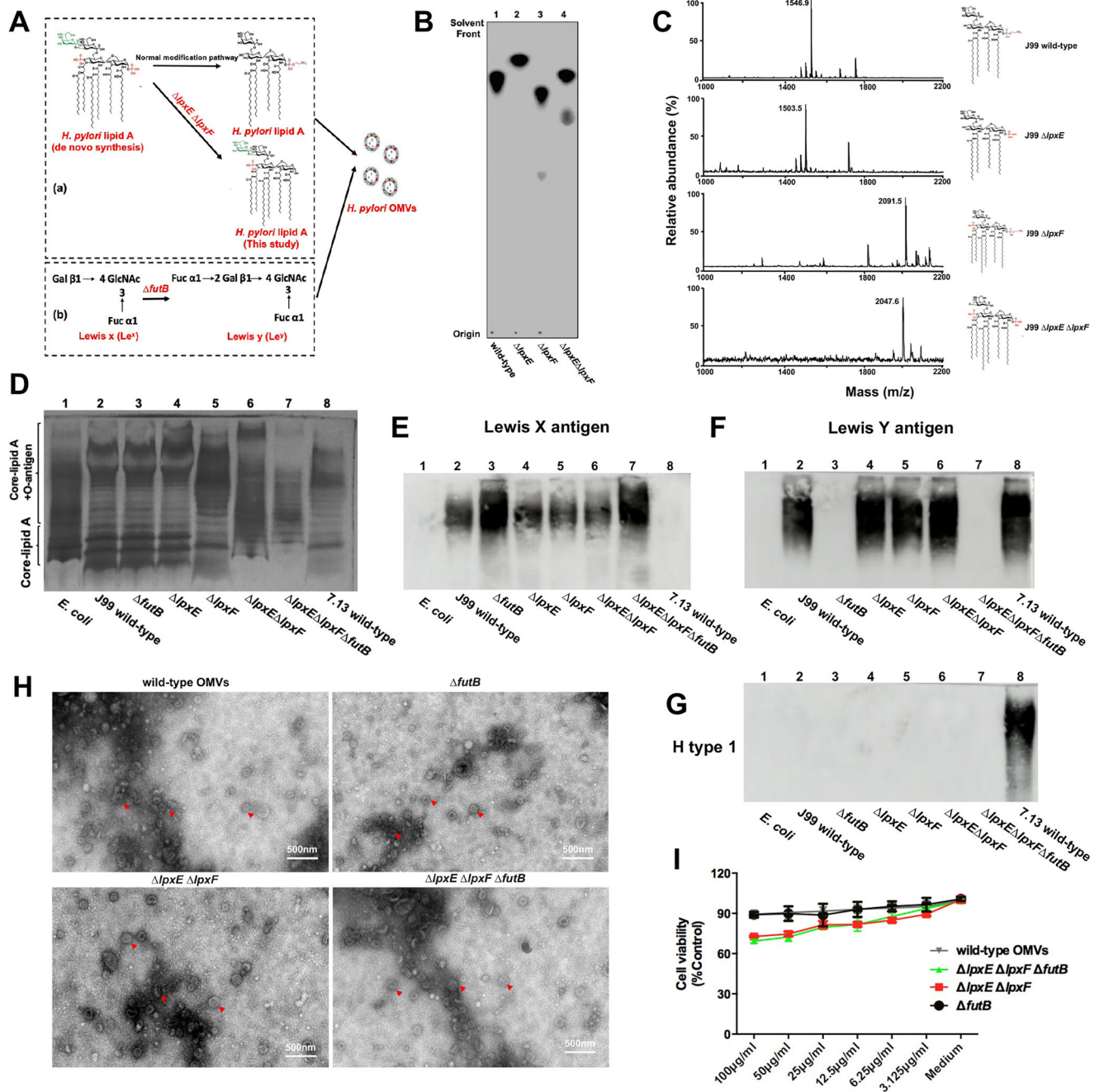


FIGURE 1 | Construction and characterisation of recombinant *H. pylori* OMVs vaccine vector. (A) Modification of the lipid A structure of *H. pylori* by knocking out the *lpxE* and *lpxF* genes. (B) Detection of radiolabelled lipid A substrate by thin-layer chromatography (TLC). (C) Identification of the lipid A structure of individual strains with ESI-MS. The peak value of 1546.7 m/z corresponds to the wild-type tetra-acylation structure (lack of 4' phosphate, while the 1' phosphate group is acylated), 1503.5 corresponds to tetraacylated 1' phosphorylated lipid A, 2091.5 corresponds to hexa-acylated 4' phosphorylated lipid A, and 2047.6 corresponds to hexa-acylated bisphosphorylated lipid A. (D) Detection of modified lipid A by silver staining and SDS-PAGE. (E) Analysis of Lewis X antigen with modified O antigen by Western blotting. LPS of wild-type J99 as positive control. (F) Analysis of Lewis Y antigen with modified O antigen by Western blotting. LPS of wild-type J99 as positive control. (G) Validation of the modified O antigen by western blotting with H type 1 antigen serum as the probe and LPS of wild type 7.13 as the positive control. (H) Observation of the morphology of LPS-modified OMVs by the transmission electron microscope. (I) Assessment of the cytotoxicity of OMVs. RAW 264.7 macrophages were treated with different doses of wild-type *H. pylori* and mutant OMVs, with the cell lysis group as a quality control. Data were expressed as mean \pm standard deviation (SD), and means were compared using the least significant difference test. * p < 0.05 and ** p < 0.01 represent differences between relevant groups.

3.2 | OMVs With Modified LPS Structure Induce Humoral and Mucosal Immunity and Provide Effective Protection Against *H. pylori* Infection

To verify the ability of the modified OMVs to bind to TLR4 and activate the immune response in vitro. LPS from each strain was purified and used to activate HEK-293 cells modified to express human and murine TLR4-MD2 receptors, respectively, and their absorbance was measured. The ability to activate TLR4 of $\Delta lpxE \Delta lpxF \Delta futB$ mutants and the double $\Delta lpxE \Delta lpxF$ mutants was significantly enhanced compared with the wild type and showed significant specificity for the human TLR4-MD receptor ($p < 0.01$) (Figure 2A,B), which indicates that the modified LPS can effectively activate human TLR4. Further, the purified OMVs were incubated with DC cells for 12 h, with LPS of *E. coli* as a positive control and a blank treatment group as negative control. It was observed that the ability of $\Delta lpxE \Delta lpxF \Delta futB$ mutants to stimulate DC cell maturation was not significantly different from that of the wild-type strain, indicating that the modified OMVs remain well antigenic (Figure 2C).

To investigate the immunogenicity of the OMVs with modified LPS, mice were orally inoculated with the OMVs. All mice did not show any abnormalities and were in good health during immunisation. The biological distribution of OMVs in different groups of mice demonstrated that LPS modification did not affect the distribution of OMVs entering the mouse by gavage. Fluorescence signals were observed in the stomach, kidney and intestines of mice at 3–6 h post-entry through Cy7-labelled OMVs, and the fluorescence slowly quenches after 12 h (Figure S2A,B). Immunofluorescence has the strongest intensity on the third day, and then the fluorescence of OMVs in the stomach and intestines of mice in each group gradually weakens over time (Figure S2C,D). Interestingly, the $\Delta lpxE \Delta lpxF \Delta futB$ mutant group showed the strongest in vivo fluorescence in the stomach after 24 h and indirect-immunofluorescence in the stomach and small intestines after 7 days, indicating that the retention time of OMVs in the body can also be a key factor in inducing efficient immune protection. Moreover, blood samples and gastric tissues were collected from the mice at Weeks 4 and 8 after initial immunisation (Figure 2D). The OMVs-induced specific antibodies against different antigens were measured by ELISA. The results showed that the serum immunoglobulin levels in the $\Delta lpxE \Delta lpxF \Delta futB$ mutant group and the $\Delta lpxE \Delta lpxF$ mutant group were significantly higher than those in the wild-type group ($p < 0.01$) (Figure 2E,F). In addition, the serum and gastric mucosal sIgA levels in the $\Delta lpxE \Delta lpxF \Delta futB$ mutant group were significantly different from those in the $\Delta lpxE \Delta lpxF$ mutant group ($p < 0.01$) (Figure 2G,H). We also tested the levels of antibodies against inactivated whole cell antigens, and the results were consistent with the trend between different groups and the previous results (Figure S3). These data suggest that the modified OMVs were able to induce better humoral and mucosal immune responses.

Ten weeks after the initial immunisation, the mice were orally inoculated with highly virulent *H. pylori* 7.13, and gastric tissues were collected for urease assay and bacterial load measurement to evaluate the immune-protective efficacy of the modified OMVs against *H. pylori* infection. The urease activity in gastric tissues from the mice immunised with the mutant OMVs (both the $\Delta lpxE$

$\Delta lpxF \Delta futB$ mutant group and the $\Delta lpxE \Delta lpxF$ mutant group) was significantly lower than that of the wild type ones ($p < 0.01$) (Figure 2I). In addition, *H. pylori* isolated from the gastric tissues was cultured and the bacterial load was determined. The colony count results were generally consistent with the results of urease activity, and the $\Delta lpxE \Delta lpxF \Delta futB$ mutant group and the $\Delta lpxE \Delta lpxF$ mutant group were significantly lower than the wild-type group ($p < 0.01$) (Figure 2J). These results suggest that the modified OMVs could induce a protective immunity against *H. pylori* infection.

To better understand the molecular mechanisms of OMVs-induced immune-protection, cytokine levels in the supernatants of MLN cells and splenocytes harvested from mice and stimulated by OMP antigen from *H. pylori* 7.13 strain were measured. IFN- γ and IL-12 are known to be indicators of Th1 polarisation response, whereas IL-4 and IL-13 are known to be indicators of Th2 polarisation response (Song et al. 2020), and IL-17 is an indicator of Th17 polarisation (Dewayani et al. 2021). The results showed that the OMVs from the $\Delta lpxE \Delta lpxF \Delta futB$ mutant group and the $\Delta lpxE \Delta lpxF$ mutant group significantly increased the cytokine production levels. In MLN cells, cytokine levels were found to be significantly higher in the $\Delta lpxE \Delta lpxF \Delta futB$ mutant group and the $\Delta lpxE \Delta lpxF$ mutant group than those in the wild-type group ($p < 0.01$) (Figure S4). Specifically, the $\Delta lpxE \Delta lpxF \Delta futB$ mutant group produced significantly higher levels of IL-17 compared to the $\Delta lpxE \Delta lpxF$ mutant group ($p < 0.01$). Similarly, for splenocytes, cytokine levels were significantly higher in the $\Delta lpxE \Delta lpxF \Delta futB$ mutant group and the $\Delta lpxE \Delta lpxF$ mutant group than in the wild-type group ($p < 0.01$). In addition, the $\Delta lpxE \Delta lpxF \Delta futB$ mutant group produced significantly higher Th1-, Th2- and Th17- indicated cytokine levels compared to the $\Delta lpxE \Delta lpxF$ mutant group ($p < 0.01$). From the perspective of cytokine levels representing different types of immune responses, the level of IL-17 produced by LPS-modified OMVs immunised mice is significantly higher than that of other types of cytokines. Taken together, these data demonstrate that the LPS-modified OMVs are able to induce Th1/Th2/Th17 mixed immune response, with Th17 being predominant.

In addition, we used OMPs and OMVs derived from the J99 strain as stimulating antigens to determine the cytokine production levels from MLN cells and splenocytes in the immunised mice, and to evaluate the induction of immune response types by genetically engineered OMVs derived from *H. pylori* J99 strain as a background strain. Our data showed that using homologous OMPs and OMVs as stimulation antigens can induce higher levels of different types of cytokines from MLN cells and splenocytes in immunised mice, and the trend in different experimental groups is consistent with previous results (Figures S5 and S6), indicating that using OMPs derived from 7.13 strain as antigens in this study can effectively reflect the immune mechanisms between different experimental groups.

3.3 | Genetically Engineered *H. pylori* OMVs Successfully Delivered *H. pylori* UreB, VacA and CagA Antigens

Utilising the Hbp autotransporter platform, we replaced the side domains d1 and d2 of the passenger domain with UreB and

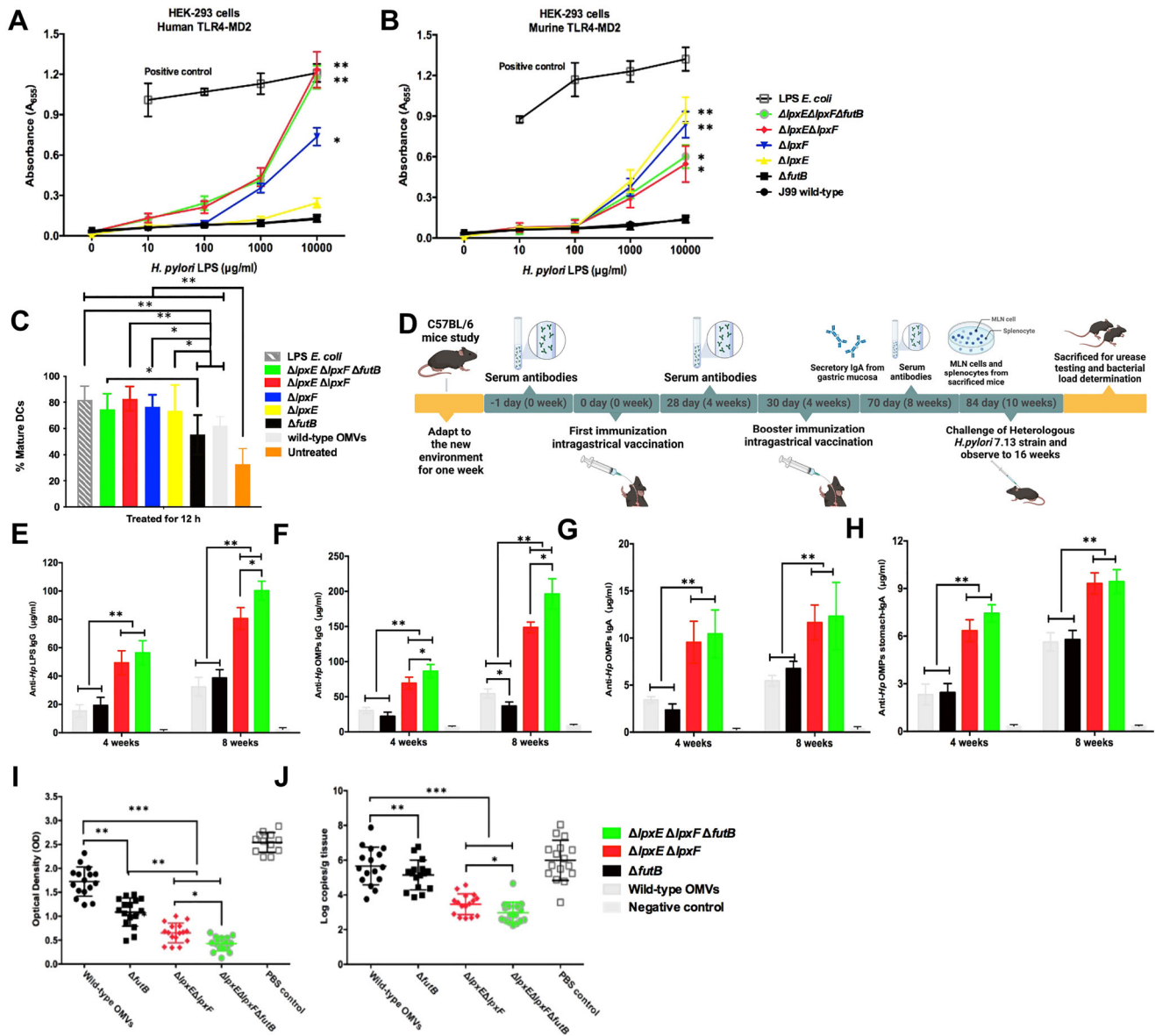


FIGURE 2 | Characterisation of immune responses by OMV with wild-type and modified LPS in vitro and in vivo. (A and B) Activation of TLR4 in HEK-293 cells stably transfected with either human (A) or murine (B) TLR4-MD2. TLR activation was monitored colour metrically using a secreted alkaline phosphatase (SEAP) reporter gene placed under the control of an NF- κ B inducible promoter. Highly purified LPS from the indicated strains of *H. pylori* was added to each well in triplicate at 0, 10, 100, 1000 and 10,000 μ g/mL. Values are the mean of results from triplicate wells plus the standard deviation. LPS of *E. coli* was used as positive control. (C) Promotion of DC cell maturation by OMVs. Immature DC cells were co-incubated with purified OMVs for 12 h. The percentage of mature DC cells in each group was counted, and the mean was calculated in triplicate. *E. coli* LPS was used as a positive control. (D) A schematic diagram showing the experimental procedures for vaccination of the mice. In brief, mice (6 weeks old, 16–22 g) were divided into five groups and immunised with OMVs vaccine by gavage. Booster immunisation was performed after 4 weeks. Blood samples were repeatedly collected, and then a lethal dose of *H. pylori* 7.13 was administered orally after booster immunisation. The concentration of antibodies was determined at Weeks 4 and 8 after the first immunisation. Animal experiments were performed twice, and the data were combined for analysis. Concentrations of anti-LPS IgG (E), anti-OMPs IgG (F) and IgA (G) in serum and anti-OMPs IgA (H) secreted by gastric mucosa were measured by enzyme-linked immunosorbent assay (ELISA) at Weeks 4 and 8, respectively. Gastric tissues of immunised mice were taken, washed in PBS buffer, and urease activity and bacterial load were determined. (I) Urease activity in gastric homogenates of mice was measured 4 weeks after attacking the infection. (J) *H. pylori* colony counts in gastric homogenates. Data were expressed as mean \pm standard deviation (SD), and means were compared using the least significant difference test. * $p < 0.05$ and ** $p < 0.01$ represent differences between relevant groups.

VacA antigens, respectively, and inserted the CagA antigen into the position of side domain d4. This allowed for the successful expression of the three antigens on the outer surface of OMVs (Figure 3A) (Jong et al. 2012). Furthermore, we introduced targeted antigenic proteins onto the surface of OMVs generated

by various knockout strains using the Hbp autotransporter system (Figure 3B) (Liu et al. 2016). SDS-PAGE and western blot analyses were conducted to verify the expression of the three antigenic proteins. Specific bands were observed in the corresponding regions of the protein extracted from strains containing UreB,

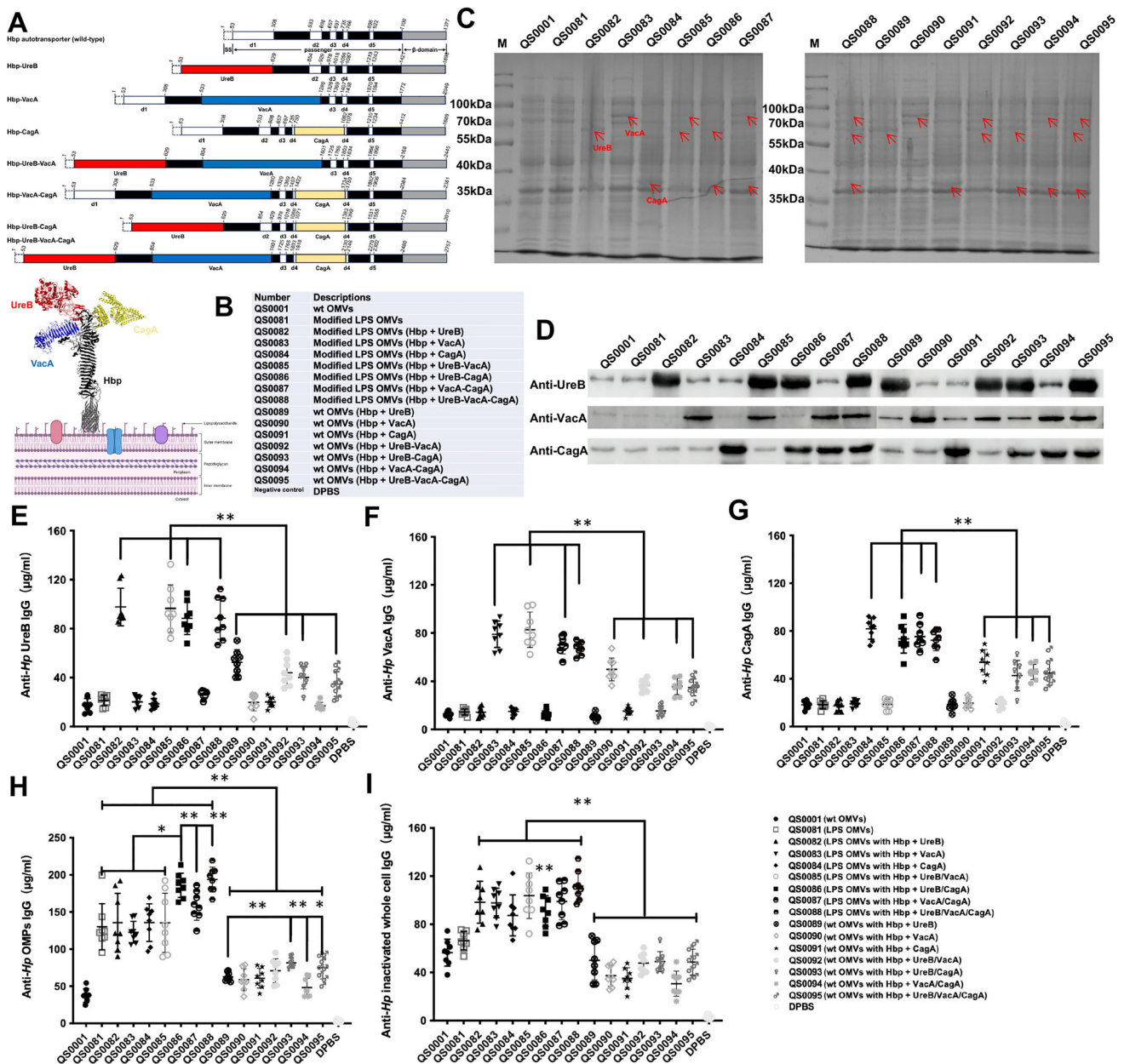


FIGURE 3 | Construction, heterologous antigen protein characterisation, and quantities of genetically engineered OMVs. (A) A diagram showing the generation of OMVs expressing UreB, VacA and CagA alone or co-expressing these three antigens simultaneously using the Hbp autotransporter platform. In brief, the side domains d1 and d2 of the passenger domain were replaced by antigens UreB and VacA, respectively, and the CagA antigen was inserted into side domain d4. A cartoon showing Hbp-mediated UreB, VacA and CagA ligation to the surface of outer membrane vesicles. The protein structures were generated using PyMOL. (B) A list of the OMVs used in this study. (C) SDS-PAGE analysis showing that UreB, VacA and CagA were successfully introduced into the OMVs derived from the *H. pylori* $\Delta lpxE \Delta lpxF \Delta futB$ mutant strain. The molecular weights of UreB, VacA and CagA proteins are located in the regions indicated by the protein markers of 55–70 kDa, 70–100 kDa and 35–40 kDa, respectively, as indicated by the red markers. (D) The western blot shows the protein bands that are consistent with the UreB antigenic protein in all strains, indicating its successful introduction into the corresponding mutant strain. Furthermore, different combinations of antigenic proteins UreB, VacA and CagA were introduced into OMVs, and their serum was collected 4 weeks after the final immunisation to detect antigen-specific IgG levels (E–G). The levels of anti-OMPs IgG and anti-inactivated whole cell IgG were also evaluated (H and I). All antibodies were measured by ELISA. The means were compared using the least significant difference test. * $p < 0.05$ and ** $p < 0.01$ represent differences between relevant groups.

VacA and CagA, confirming the successful import of the proteins into the specific knockout bacteria (Figure 3C,D).

To assess the impact of our knockout strategy on the quantity of OMVs released by the strains, we quantified the levels of

OMV secretion in each group. Notably, a modest increase in *H. pylori* OMV production was observed when genes related to LPS synthesis were disrupted (Figure S7). To identify the optimal combination of *H. pylori* antigenic proteins, we incorporated various combinations of UreB, VacA and CagA into OMVs derived from

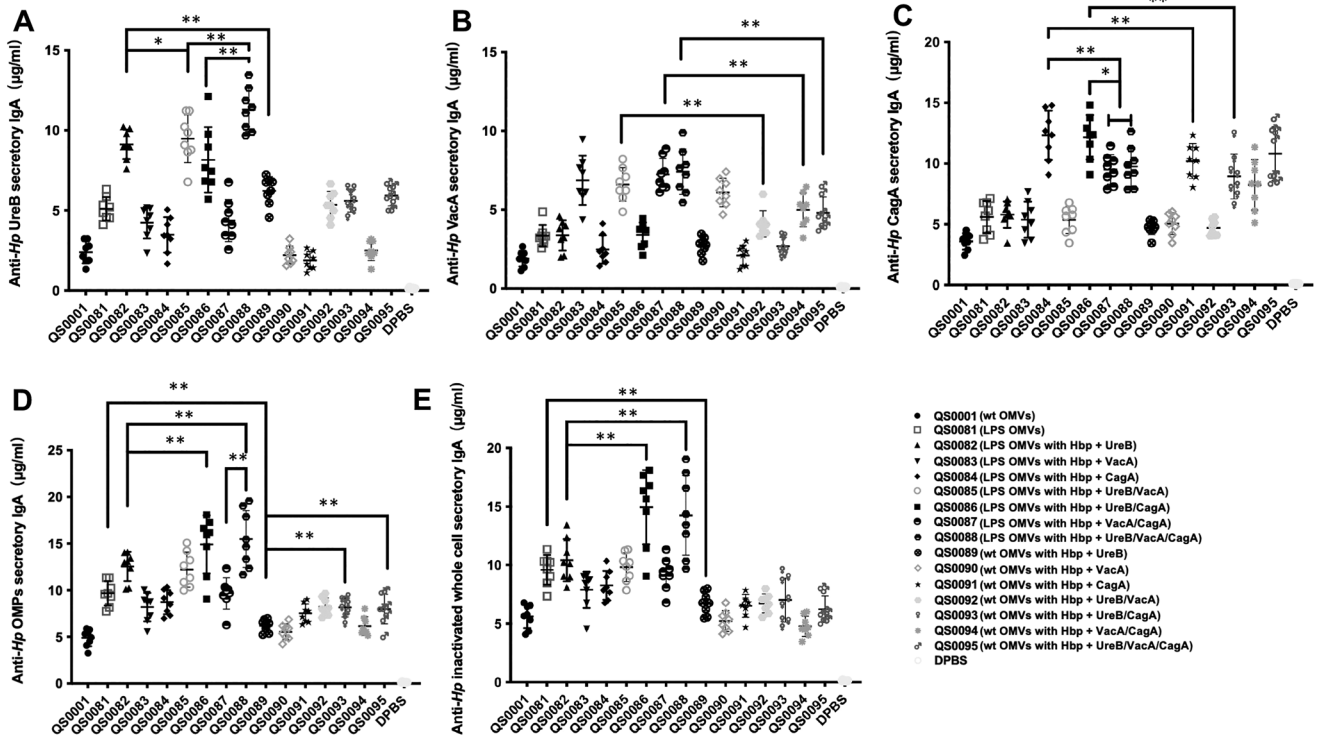


FIGURE 4 | Identification of mucosal immune response induced by OMVs delivering *H. pylori* antigens. Concentrations of anti-UreB, VacA and CagA secretory IgA (A, B and C), and anti-OMPs secretory IgA (D) and anti-inactivated whole cells secretory IgA (E) secreted by the gastric mucosa were measured by enzyme-linked immunosorbent assay (ELISA) at Week 8, respectively. The means were compared using the least significant difference test. * $p < 0.05$ and ** $p < 0.01$ represent differences between relevant groups.

an *H. pylori* strain with modified LPS. Following immunisation with different combinations of OMVs and *H. pylori* antigens, a significant increase in corresponding IgG levels was observed in mice ($p < 0.01$; Figure 3E–G). Notably, antibody levels varied among groups immunised with different antigen combinations, with IgG levels against UreB, VacA and CagA induced by OMVs with a modified LPS structure being remarkably higher compared to other groups (Figure 3E–G), demonstrating the design strategy of utilising OMVs to deliver multiple *H. pylori* antigens is feasible. At the same time, we also measured the levels of IgG antibodies against OMPs and inactivated whole cell antigens in groups delivering different antigens. These results showed that the modified OMVs could serve as vectors to deliver antigens and induce higher levels of IgG antibodies. Of note, the combination of various antigens may induce different levels of anti-OMPs IgG antibodies (Figure 3H,I).

3.4 | Genetically Engineered OMVs Delivering *H. pylori* UreB, VacA and CagA Antigens Could Induce Strong Mucosal Immune Responses

The gastric secretory type mucosal immunity has been suggested to be crucial for resisting *H. pylori* infection. Therefore, we evaluated whether the OMV vector enhances the ability to stimulate the production of secretory IgA after delivering *H. pylori* antigens. The quantitative ELISA results demonstrated that the recombinant OMV vaccine delivering the corresponding antigen could induce the production of IgA antibodies against specific antigens, which once again confirms the successful construction

of the OMV-based antigen delivery strategy (Figures 4A–C and S8). At the same time, the modified OMVs may serve as vectors for delivering antigens and induce higher levels of serum IgA and gastric mucosal secretory IgA than wild-type OMVs (Figures 4A–C and S8).

In addition to measuring the serum and secretory IgA levels against specific antigens in immunised mice, we also evaluated the serum and secretory IgA levels against OMPs or whole bacterial antigens in mice from different immune groups, in order to understand the effect of mucosal immunity against *H. pylori* infection. These results showed that the modified OMVs delivering UreB, VacA and CagA, as well as recombinant vaccines delivering UreB and VacA, exhibited higher levels of secretory IgA compared to other recombinant vaccines delivering two antigens (Figure 4D,E). Of note, in terms of serum IgA, the modified OMVs as antigen delivery vectors induced significantly higher antibody levels than the wild-type ones (Figure S8), which suggested that using the OMVs with modified LPS as vectors for delivering *H. pylori* antigens may induce stronger humoral immune responses against *H. pylori* infection.

3.5 | Genetically Engineered OMVs Delivering *H. pylori* UreB, VacA and CagA Antigens May Induce Protective Immunity Against *H. pylori* Infection

To further evaluate the protective immunity induced by the modified OMVs bearing various *H. pylori* antigens, we first tested the bacteria opsonisation and phagocytosis activities by the sera from

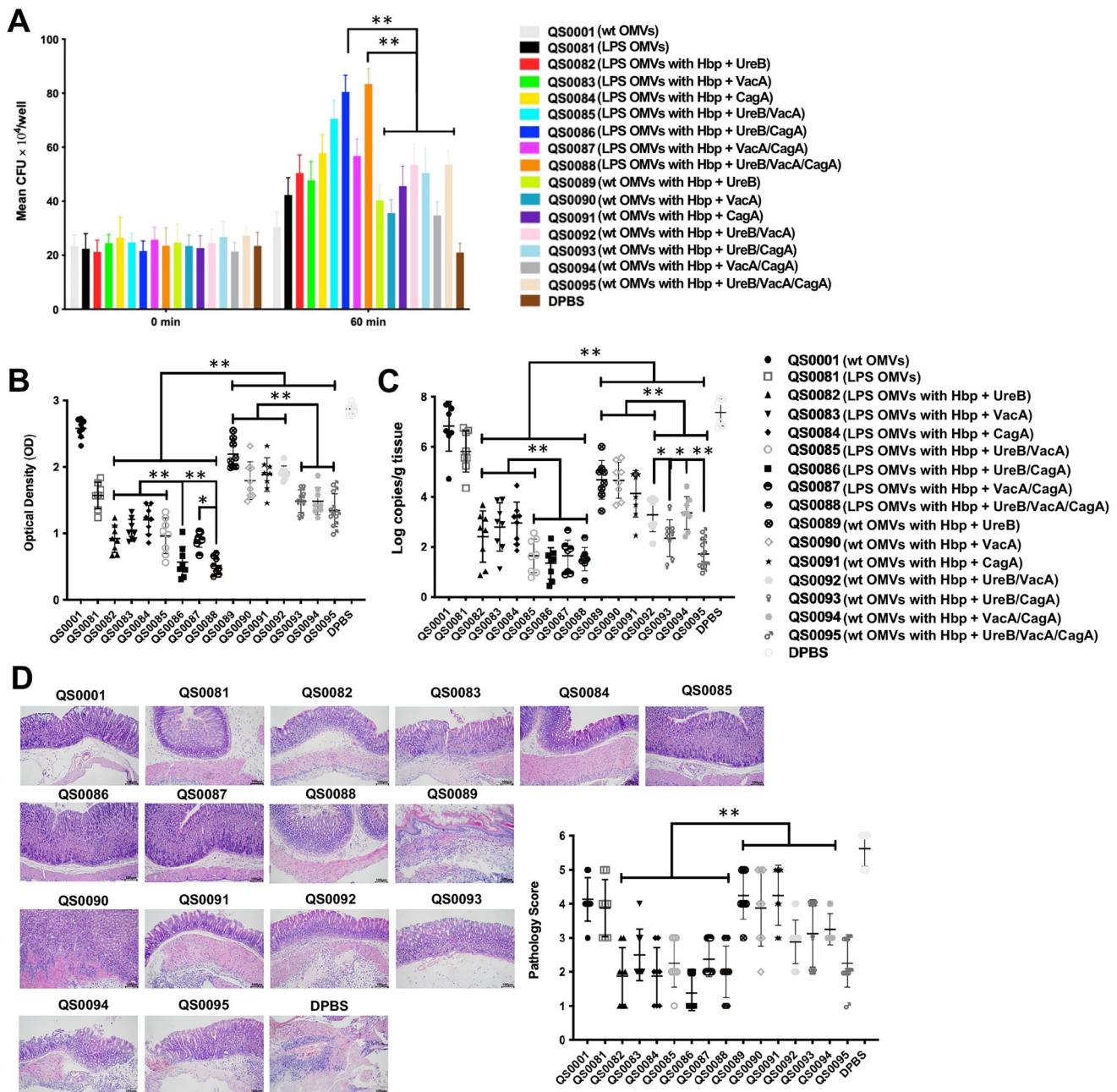


FIGURE 5 | Protective immunity against *H. pylori* induced by OMVs derived from different antigen combination strategies. (A) Opsonisation of sera from mice immunised with OMVs delivering various *H. pylori* antigens in vitro. (B) Urease activity in gastric tissue homogenates from mice immunised with OMVs delivering various antigen combinations was assessed 2 weeks after the challenge infection. (C) *H. pylori* colony counts in gastric tissue homogenates were quantified to determine bacterial loading. (D) Histopathological examinations of gastric mucosa in mice immunised with various OMVs, and the corresponding pathology score of various groups were shown. The means were compared using the least significant difference test. * $p < 0.05$ and ** $p < 0.01$ represent differences between relevant groups.

the mice immunised with the OMV vaccine using an isolated macrophage model. We observed significantly enhanced bacterial uptake in the groups immunised with the modified OMVs delivering UreB and CagA or UreB, VacA and CagA (Figure 5A), indicating that the sera from the mice immunised with both the antigen combinations displayed enhanced opsonisation and phagocytosis activities of *H. pylori* by macrophages. Of note, there was no significant change in body weight among different groups of mice during the 6 weeks of infection study (Figure S9). The mice were subsequently sacrificed and their gastric tissues were

collected for detection of *H. pylori* infection by testing the urease activity and bacterial load. Being consistent with the previous results, the urease activities and bacterial loads were notably lower in the mice immunised with antigen-presenting OMVs than the negative control mice, indicating that the modified OMVs induced significant protection against *H. pylori* infection. In particular, the urease activity was remarkably lower in the gastric tissues of mice immunised with QS0086 (UreB-CagA) and QS0088 (UreB-VacA-CagA) than that with other antigen combinations (Figure 5B). As expected, the bacterial loading

results were consistent with the urease activity results. Compared with other experimental strains, the QS0085, QS0086, QS0087 and QS0088 strain reduced the bacterial loading in the mice stomach tissues (Figure 5C). The histopathological examinations of stomach tissues from various groups were scored and the gastric mucosa of the mice immunised with OMVs derived from QS0086 strain showed no abnormalities (Figure 5D). These findings suggested that the modified OMVs secreted by the knockout strain delivering UreB and CagA, or UreB, VacA and CagA antigens may induce protective immunity against *H. pylori* infection.

3.6 | Genetically Engineered OMVs Delivering *H. pylori* Antigens May Induce Th1/Th2/Th17-Based Immune Responses

To further understand the cellular immunity induced by various OMVs in mice, we examined the levels of cytokines produced by mouse splenocytes from different vaccination groups described above. We quantified the levels of the cytokines IFN- γ , IL-4, IL-6, IL-12 (p40), IL-13 and IL-17 in mouse MLN cells and splenocytes after antigen stimulation by ELISA. The results showed that the levels of IFN- γ , IL-4, IL-12 (p40) and IL-13 were significantly higher in OMV-immunised groups delivering the UreB, VacA and CagA (QS0088) or UreB and CagA (QS0086) than in the control groups, indicating that OMV immunisation triggered both Th1 and Th2 cellular immune responses in mice (Figure 6A–H). Furthermore, the IL-17 levels were markedly higher in the modified OMV-immunised group than in the other groups, indicating that antigen-presenting OMVs secreted by LPS-modified strains effectively induced specific T helper 17 (Th17) cellular immune responses in mice (Figure 6H,J). We also measured the level of pro-inflammatory cytokine IL-6 in MLN cells and splenocytes in each knockout group, and it increased much lesser degree compared to other cytokines described above.

In mice, IgG₁ and IgG_{2c} levels are well-established indicators of Th1 and Th2 responses, respectively. To gain insight into the immune mechanisms underlying the response to OMVs delivering *H. pylori* antigenic proteins, it is crucial to clarify the type of immune response induced. Therefore, we employed quantitative ELISA to assess and compare serum IgG₁ and IgG_{2c} levels in immunised and control mice, thereby evaluating the bias of the immune response. Overall, LPS-modified OMVs used for delivering the *H. pylori* antigens showed significantly higher levels of IgG₁ and IgG_{2c} induction compared to wild-type OMVs, except for the groups measured with OMPs as the coating antigen (Figure S10). These data indicate that LPS-modified OMVs have a stronger ability to induce Th1 and Th2 type immune responses than wild-type OMVs. In addition, the ratio of IgG₁/IgG_{2c} in the groups of *H. pylori* antigen-presented LPS modified OMVs was higher than 1, indicating that it induced a Th1/Th2 mixed immune response with Th2 being predominant (Figure S9C,F). In terms of delivering different *H. pylori* antigens, the experimental groups of LPS modified OMVs delivering UreB and CagA (QS0086) and UreB, VacA and CagA (QS0088) showed higher Th1 and Th2 type immune responses compared to other antigen combination experimental groups, which is consistent with the results of cytokine detection. In addition, the induction of IgG₁ and IgG_{2c} levels against the *H. pylori* antigens in mice

immunised with recombinant OMV vaccine was also detected. The immunised group of OMVs delivering the corresponding antigen protein was also able to induce higher levels of IgG₁ and IgG_{2c}, and exhibited a Th1/Th2 mixed immune response (Figure S10). However, the OMVs that did not deliver the corresponding antigen protein showed similar results to previous levels of IgG and IgA (Figure 3), and did not produce high levels of IgG₁ and IgG_{2c} (Figure S11).

To further assess the impact of the vaccine, we employed flow cytometry to analyse and compare the levels of CD4⁺ and CD154⁺ T lymphocytes, as well as CD4⁺ CD154⁺ T lymphocytes secreting IFN- γ or IL-17A in mice stimulated with various antigen combinations. CD154 is used as a cell membrane molecule marker for antigen-specific activation of CD4⁺ T lymphocytes, and is essential for the T cell-dependent activation of B lymphocytes. Immunisation with LPS-modified OMVs serving as vectors for *H. pylori* antigenic proteins resulted in a significant increase in the levels of mouse-specific CD4⁺ CD154⁺ T cells, CD4⁺ CD154⁺ IFN- γ ⁺ T cells and CD4⁺ CD154⁺ IL-17A⁺ T cells compared to wild-type OMVs. These findings provide further evidence of the vaccine's efficacy (Figure 6L–N). Additionally, the QS0086 and QS0088 strains demonstrated a higher increase compared to other strains, reinforcing the notion that protection against *H. pylori* infection is mediated by Th1/Th2/Th17 mixed immune responses with Th17 being predominant.

4 | Discussions

Immune escape of *H. pylori* is an important challenge in its current vaccine development. LPS is the central component of the outer membrane of Gram-negative bacteria and plays a key role in bacterial pathogenesis (Whitfield and Trent 2014). For *H. pylori*, modification of the LPS structure is an important mechanism for the immune escape phenomenon, which is achieved by generation of tetraacylated lipid A via dephosphorylation and acylation to reduce binding to TLR4 as well as by modification of O antigen to mimic human serum Le antigen via a series of rockwell glycosyltransferases such as FutB (Maldonado et al. 2016; Rubin and Trent 2013). The specific process of *H. pylori* modification of lipid A has been elucidated in detail, by which *lpxE* cleaves the 1' phosphate group, *eptA* is acylated by the addition of ethanolamine phosphate (PE) at the 1' position, and *lpxF* is involved in the removal of the 4' phosphate group (Cullen et al. 2011). According to the known specific process of LPS modification and related regulatory genes, we successfully blocked the modification of LPS structure by *H. pylori* through knocking down *lpxE*, *lpxF* and *futB*, and subsequently constructed the lipid A structure with six fatty acid chains, and disrupted the molecular mimicry of O antigen to Lewis antigen. The antigenicity of the modified LPS was then examined by stably transfecting HEK-293 cells with human or mouse TLR4-MD2.

Gastric epithelial cells expressing TLRs and the pattern recognition receptors (PRRs) on their membranes are the first line of defence against *H. pylori* infection (Zhang et al. 2024). Bacterial antigens are able to bind to specific TLR families to activate the innate immune response (D'Oro and O'Hagan 2024). For example, the hexa-acylated lipid A binds to TLR4-MD2, which in turn causes a strong inflammatory response (Maldonado et al.

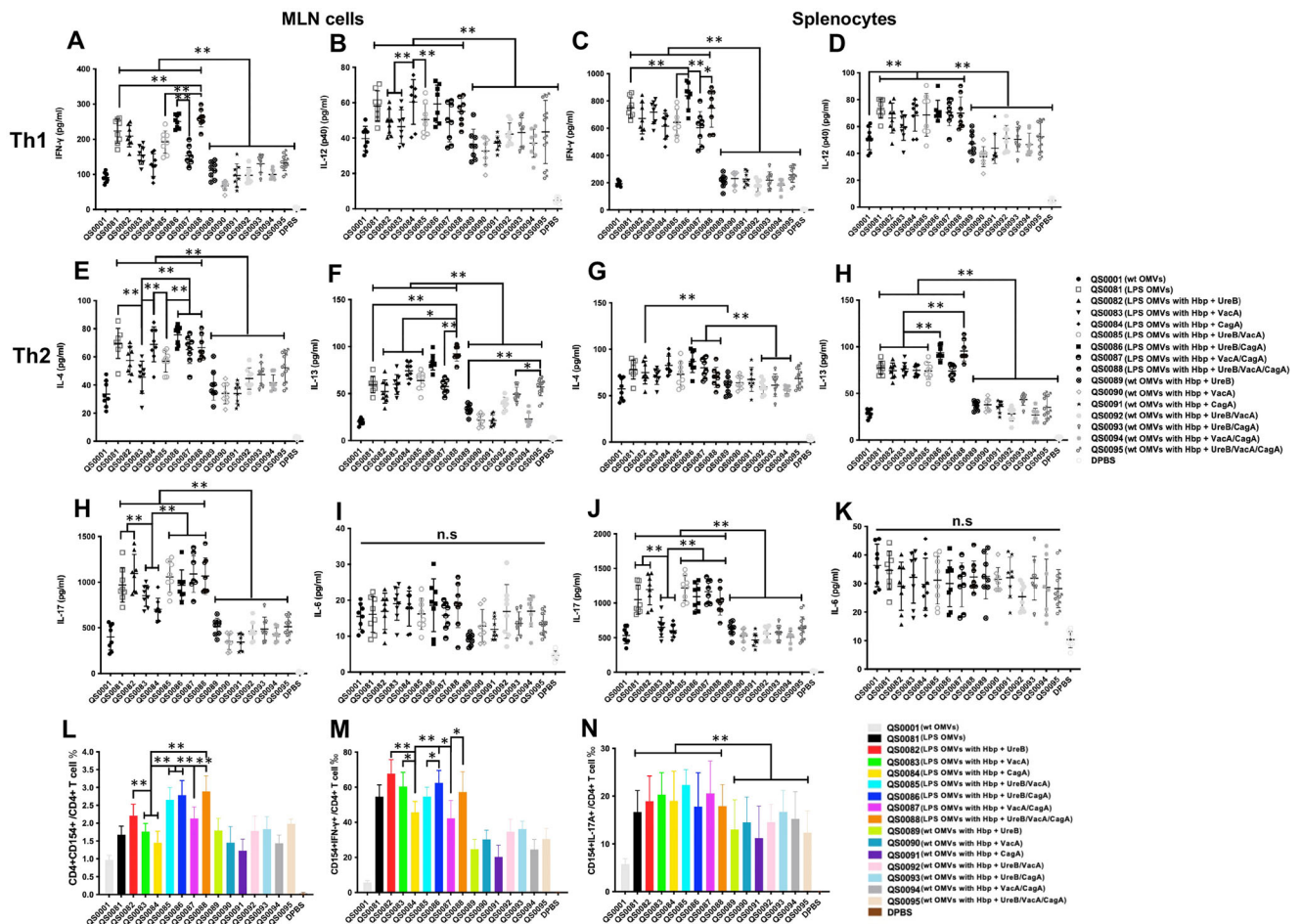


FIGURE 6 | Immune regulatory mechanisms in mice immunised with OMVs delivering various *H. pylori* antigens. The levels of cytokines secreted by MLN cells and splenocytes. IFN- γ (A and C), IL-12 (B and D), IL-4 (E and G), IL-13 (F and H), IL-17 (H and J) and IL-6 (I and K) levels secreted by MLN cells and splenocytes from mice immunised with OMVs delivering various *H. pylori* antigens. MLN cells and splenocytes were isolated from mice after the final immunisation and cultured with outer membrane proteins from *H. pylori* for 24 h. IFN- γ , IL-12, IL-4, IL-13, IL-17 and IL-6 levels in culture supernatants were determined using specific ELISAs. For evaluation of antigen-specific CD4⁺ T cell immune responses, 8 weeks after the *H. pylori* challenge, the spleens were collected from mice to prepare a single-cell suspension. After staining with intracellular cytokines, flow cytometry was used to determine the proportion of CD4⁺ CD154⁺ T cells (L), CD154⁺ IFN- γ ⁺ T cells (M) and CD154⁺ IL17A⁺ T cells (N) in total CD4⁺ T cells. The data are presented as mean \pm SD. The means were compared using the least significant difference test. * p < 0.05 and ** p < 0.01 represent differences between relevant groups.

2016). As previously mentioned, the wild-type *H. pylori* LPS does not bind to TLR4-MD2, whereas the genetically modified LPS from the mutant strains can be recognised by TLR4 (Figure 2A,B). Specifically, we obtained a lipid A structure of *H. pylori* with six hydrophobic acyl chains and two phosphate groups by simultaneously knocking out *lpxE* and *lpxF*, but its structure still differs from that of *E. coli* lipid A in terms of carbon base length. This can also partially explain why the ability of LPS to activate human TLR4 is weaker compared to *E. coli*. Moreover, our data revealed the differential activation of human and mouse TLR4 by the same lipid A structure. We may explain this from the following two aspects. First, the ability of human and murine TLR4 to recognise lipid A is different. Previous reports have demonstrated that human TLR4 needs to recognise the full structure of lipid A (six hydrophobic acyl chains and suitable phosphate moieties), while murine TLR4 can recognise multiple structures of lipid A (tetra-acylated, penta-acylated lipid A) (Alexander-Floyd et al. 2022; Li et al. 2016). That is why lipid A, with knocking out

lpxE does not activate human TLR4 but could trigger activation of murine TLR4. The lipid A structure formed by knocking out *lpxF* contains complete six fatty acid chains but lacks phosphate groups, thus maintaining the same level of TLR4 activation in humans and mice. Second, the natural host of *H. pylori* infection is humans rather than mice, indicating that *H. pylori* lipid A might be less suitable for activating TLR4 in mice and maintaining the immune escape of the bacteria in mice (Cullen et al. 2011). Taken together, we have obtained a lipid A structure of *H. pylori* that can effectively activate murine and human TLR4 through genetic engineering modification and making it a potential candidate for vaccine antigens.

In addition, antigen delivery systems can affect the immune response both qualitatively and quantitatively. Therefore, antigen presentation is crucial for the success of vaccine development, especially for *H. pylori* (Pardi and Krammer 2024). Indeed, we found that the OMVs with modified LPS could stimulate the

maturation of mouse-derived DC cells (Figure 2C), which, as the most efficient antigen-presenting cells, were able to significantly activate both naive and memory immune responses (Sabado et al. 2017).

Of note, the OMVs derived from the knockout of *lpxE* and *lpxF* alone can also induce the maturation of DC cells derived from mice, and are even higher than the $\Delta lpxE \Delta lpxF$ mutant OMVs (Figure 2C). This finding is consistent with the ability of lipid A from these mutant strains to activate murine TLR4, indicating a correlation between DC cell maturation and TLR4 activation. However, we did not choose to knock out *lpxE* and *lpxF* separately for the subsequent animal experiments because we consider the following points: (1) *H. pylori* is a human pathogen and (2) the *lpxE* and *lpxF* double knockout strains can induce very high activation of human TLR4, which may become a potential strain for subsequent vaccine development.

Production efficiency and safety are crucial for vaccine development. We demonstrated by nanoparticle tracking analysis that the knockdown of *lpxE*, *lpxF* and *futB* did not affect the particle size and yield of OMVs (Figure S1), ensuring the production efficiency of these vaccine candidates. The modified OMVs showed some toxic effects on RAW264.7 cells at higher concentrations (Figure 1I), which may be associated with the enhanced antigenicity of LPS after gene editing. However, at lower concentrations, there was no significant toxic effect, and the safety of the vaccine could be guaranteed under the condition of moderate control of the LPS concentration contained in the vaccine.

We also found that mice immunised with $\Delta lpxE \Delta lpxF \Delta futB$ mutant OMVs produced higher levels of serum IgG, IgA and gastric sIgA than the wild-type OMVs ($p < 0.01$) (Figure 2E–H). This suggests that OMVs with modified LPS can effectively induce humoral and mucosal immunity. Moreover, the modified OMVs as vector for delivering *H. pylori* antigens can also induce significant serum IgA and gastric mucosal secretory IgA, and antigen combinations delivering UreB, CagA and UreB, VacA and CagA can induce higher levels of mucosal immunity compared to other antigen combinations (Figure 4). Notably, sIgA, which may inhibit the binding of *H. pylori* to the surface of gastric epithelial cells and reduces its colonisation, is the most important factor in mucosal immunity against *H. pylori* infection (Srivastava et al. 2013). The modification of OMVs can significantly promote sIgA secretion, which may help to understand why the modified OMVs delivering UreB and CagA, or UreB, VacA and CagA, can provide more efficient protection against *H. pylori* infection.

Unlike the non-invasive mucosal infections, *H. pylori* infection stimulates the production of IFN- γ and IL-12 cytokines that induce Th1 responses and recruit macrophages to the site of infection (Jafarzadeh et al. 2018). Th17 cells are a third subpopulation of effector Th cells that produce cytokines such as IL-17 and play an important role in host defence against extracellular pathogens (Chandra et al. 2024). Cytokines associated with Th17 cells may exhibit protective functions in the intestinal environment (Dewayani et al. 2021). For example, in microbial colitis, the protective role of IL-17 is important for the control of oral infection with rotavirus (Ishigame et al. 2009). The mixed

Th1 and Th17 immune responses have been suggested to play an important role in the prevention of *H. pylori* infection (Li et al. 2022; Xie et al. 2021; Ghasemi et al. 2018). Activation of the Th17-biased immune response is considered an important strategy to improve the immunoprotective efficacy of vaccines, as the latter is more effective in eradicating *H. pylori* infection and preventing bacterial colonisation in the stomach (Dos Santos Viana et al. 2021, Liu et al. 2011). Our data showed that $\Delta lpxE \Delta lpxF \Delta futB$ mutant OMVs were able to significantly induce Th1 and Th17 responses ($p < 0.01$), with a predominant Th17 response ($p < 0.01$) (Figure 2). Therefore, these recombinant OMVs with modified LPS may become good vaccine candidates against *H. pylori* infection.

Of course, the IL-17-mediated protection is crucial for efficient *H. pylori* vaccines and confirms the vaccine potential of recombinant OMVs with modified LPS. However, we should also bear in mind that IL-17 responses may also promote immunopathology. Ferrara and colleagues reported that neutralising IL-17 could significantly reduce bacteraemia and systemic pro-inflammatory cytokine and chemokine levels in septic mice, and improve survival rates, indicating that the elevation of IL-17 may lead to overactivation of inflammatory responses and cause the disorders (Flierl et al. 2008). In addition, the expression of IL-17A is upregulated in the serum and tumours of gastric cancer patients, and it has been demonstrated that IL-17A can promote *H. pylori*-induced gastric carcinogenesis (Kang et al. 2023). Therefore, it is necessary to consider the excessive activation of the inflammatory response caused by vaccine immunity and the potential adverse effects. Our data demonstrated that the vaccine immunisation did not induce inflammatory activation of the gastric mucosal epithelium, and IL-6 remained at a low level (Figures 5D, 6I,K), indicating that the IL-17 response caused by the recombinant OMVs is mainly beneficial for combating *H. pylori* infection.

The OMVs vaccine candidate described above has a number of advantages: (I) Selection of the modified LPS as one of the vaccine antigen components. An ideal *H. pylori* vaccine regimen should contain a highly conserved, immunogenic antigen from all strains of *H. pylori* (Yunle et al. 2024). The lipid A structure of *H. pylori* LPS is known to be highly conserved, and a vaccine developed based on LPS may be able to provide immune protection against multiple serotypes of *H. pylori* (Cullen et al. 2011; Zou et al. 2022). One of the biggest challenges in developing a vaccine containing the *H. pylori* LPS is its weak antigenicity. We blocked the modification of LPS by knocking out several key genes, and the antigenicity of the modified LPS was significantly enhanced, making it possible to use it as a vaccine antigenic component. (II) Use of OMVs as the vaccine formulation. We have demonstrated in previous studies that OMVs of *H. pylori* are a good vaccine adjuvant with some immunogenicity of their own and can be used as a self-adjuvanted vaccine, enhancing the vaccine to stimulate the specific immune responses (Song et al. 2020). Moreover, OMV is a cell-free structure and is safer than that of conventional live attenuated vaccines (Singh et al. 2024). Indeed, in this study, we further demonstrated the safety of the OMVs vaccine. Moreover, OMV vaccines are superior to other formulations, such as purified protein vaccines, for economic reasons and in terms of stability at ambient temperatures. (III) Oral immunisation. Our previous study suggests that oral immunisation might

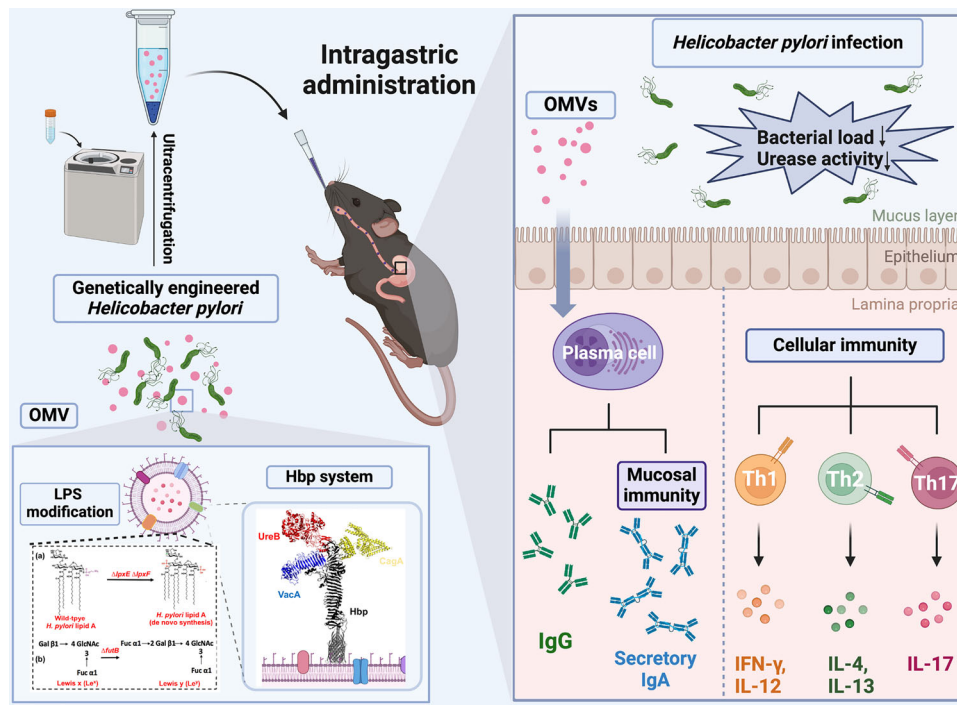


FIGURE 7 | A schematic diagram showing the mechanisms by which engineered OMVs present the *H. pylori* antigen proteins UreB, CagA and VacA as vaccines.

be the most appropriate and effective delivery strategy for *H. pylori* OMV vaccines (Li et al. 2022). Therefore, in this study, we immunised the mice by gavage, and the results demonstrated that this immunisation method could effectively induce immune protection in mice. (IV) This vaccine was able to activate Th1/Th2/Th17-balanced immune responses. (V) This vaccine was able to significantly induce gastrointestinal mucosal immunity. (VI) Given the fact that recombinant OMVs can induce IL-17-mediated protection and robust gastrointestinal mucosal immunity, it may also become a therapeutic vaccine to eradicate *H. pylori* infection in vivo. Further studies are warranted to verify the therapeutic effect of the OMV vaccine in a pre-established *H. pylori* infection model. In our study, we explored the optimal approach for introducing three key antigenic proteins of *H. pylori*—UreB, VacA and CagA—onto the surface of OMVs derived from *H. pylori* in various combinations. We found that the simultaneous incorporation of UreB and CagA into the *H. pylori* mutant strain effectively elicited robust humoral and mucosal immune responses in mice, resulting in a significant elevation of IgG and IgA levels. Previous studies have established the crucial role of IFN- γ and IL-17 in immunity against *H. pylori* infection (Zhang et al. 2022), and the expression of CD154 on activated CD4⁺ T cells has been shown to dictate the differentiation of these cells into Th1 and Th17 subsets post-immunisation (Zhong et al. 2020). Our results demonstrated that the vaccine construct significantly increased the number of CD4⁺ T cells associated with protection against *H. pylori* infection, along with elevated levels of the cytokines IFN- γ and IL-17 (Figure 6L–N). Notably, a reduction in *H. pylori* colonisation and urease activity was observed in mice following challenge experiments. Collectively, these findings indicate that our novel vaccine strategy holds promising potential for the prevention of *H. pylori* infection (Figure 7).

5 | Conclusions

In this study, we developed a novel recombinant vaccine candidate against *H. pylori* infection by knocking down the key genes of LPS modification and using the OMVs as a delivery vector for UreB, VacA and CagA antigens. Our data demonstrated that this OMV-based recombinant vaccine could induce specific humoral immune responses, including gastric mucosal immunity and a Th1/Th2/Th17 mixed immune responses with Th17 being predominant, and markedly protect the mice from *H. pylori* infection. This study established an innovative vaccine development platform for *H. pylori* and other pathogens. Finally, this OMV-based strategy may also become a powerful delivery system for protein drugs treating diseases including antibiotic-resistant bacteria infections, viral infections and even cancers.

Author Contributions

Qiong Liu: conceptualization (equal), funding acquisition (equal), project administration (equal), writing—original draft (equal). **Biaoxian Li:** investigation (equal), validation (equal). **Jinrong Ma:** methodology (equal). **Xiao Lei:** methodology (equal). **Junpeng Ma:** methodology (equal). **Yanyan Da:** methodology (equal). **Zhiyong Zhou:** methodology (equal). **Jiaqi Tao:** methodology (equal). **Xinyi Ren:** methodology (equal). **Ting Zeng:** methodology (equal). **Zhitong Xie:** methodology (equal). **Haiyan Lin:** methodology (equal). **Zihui Jin:** methodology (equal). **Yi Wan:** methodology (equal). **Liang Zhang:** methodology (equal). **Donglin Lai:** methodology (equal). **Yaping Guo:** methodology (equal). **Jing Li:** methodology (equal). **Yinpan Shang:** methodology (equal). **Lu Shen:** methodology (equal). **Ziwei Tao:** methodology (equal). **Tian Gong:** conceptualization (equal), writing—review and editing (equal). **Chengsheng Zhang:** conceptualization (lead), funding acquisition (lead), writing—original draft (equal), writing—review and editing (equal).

Acknowledgements

We thank all colleagues who provided assistance in this work. Funding was received from National Natural Science Foundation of China 82203032 and 32260193 (Qiong Liu), Project for high and talent of Science and Technology Innovation in Jiangxi “double thousand plan” jxsq2023301110 (Qiong Liu), the start-up fund from the First Affiliated Hospital of Nanchang University 500021010 (Chengsheng Zhang) and fund from School of Basic Medical Sciences, Nanchang University (Qiong Liu).

Conflicts of Interest

The authors declare no conflicts of interest.

Data Availability Statement

The datasets generated during and analysed during the current study are available from the corresponding author on reasonable request.

References

- Alexander-Floyd, J., A. R. Bass, E. M. Harberts, et al. 2022. “Lipid A Variants Activate Human TLR4 and the Noncanonical Inflammasome Differently and Require the Core Oligosaccharide for Inflammasome Activation.” *Infection and Immunity* 90: e0020822.
- Asim, M., S. K. Chikara, A. Ghosh, et al. 2015. “Draft Genome Sequence of Gerbil-Adapted Carcinogenic *Helicobacter pylori* Strain 7.13.” *Genome Announcements* 3: 10–1128.
- Chandra, V., L. Li, O. Le Roux, et al. 2024. “Gut Epithelial Interleukin-17 Receptor A Signaling Can Modulate Distant Tumors Growth Through Microbial Regulation.” *Cancer Cell* 42: 85–100.e6.
- Chen, Y., K. Jie, B. Li, et al. 2020. “Immunization With Outer Membrane Vesicles Derived From Major Outer Membrane Protein-Deficient *Salmonella Typhimurium* Mutants for Cross Protection Against *Salmonella Enteritidis* and Avian Pathogenic *Escherichia coli* O78 Infection in Chickens.” *Frontiers in Microbiology* 11: 588952.
- Cullen, T. W., D. K. Giles, L. N. Wolf, C. Ecobichon, I. G. Boneca, and M. S. Trent. 2011. “*Helicobacter pylori* Versus the Host: Remodeling of the Bacterial Outer Membrane Is Required for Survival in the Gastric Mucosa.” *Plos Pathogens* 7: e1002454.
- Daleke-Schermerhorn, M. H., T. Felix, Z. Soprova, et al. 2014. “Decoration of Outer Membrane Vesicles With Multiple Antigens by Using an Autotransporter Approach.” *Applied and Environmental Microbiology* 80: 5854–5865.
- Dewayani, A., K. A. Fauzia, R. I. Alfaray, et al. 2021. “The Roles of IL-17, IL-21, and IL-23 in the *Helicobacter pylori* Infection and Gastrointestinal Inflammation: A Review.” *Toxins (Basel)* 13, no. 5: 315.
- D’Oro, U., and D. T. O’Hagan. 2024. “The Scientific Journey of a Novel Adjuvant (AS37) From Bench to Bedside.” *NPJ Vaccines* 9: 26.
- Dos Santos Viana, I., M. L. Cordeiro Santos, H. Santos Marques, et al. 2021. “Vaccine Development Against *Helicobacter pylori*: From Ideal Antigens to the Current Landscape.” *Expert Review of Vaccines* 20: 989–999.
- Flierl, M. A., D. Rittirsch, H. Gao, et al. 2008. “Adverse Functions of IL-17A in Experimental Sepsis.” *FASEB Journal* 22: 2198–2205.
- Geijtenbeek, T. B., R. Torensma, S. J. van Vliet, et al. 2000. “Identification of DC-SIGN, a Novel Dendritic Cell-Specific ICAM-3 Receptor That Supports Primary Immune Responses.” *Cell* 100: 575–585.
- Geijtenbeek, T. B., S. J. Van Vliet, E. A. Koppel, et al. 2003. “Mycobacteria Target DC-SIGN to Suppress Dendritic Cell Function.” *Journal of Experimental Medicine* 197: 7–17.
- Ghasemi, A., N. Mohammad, J. Mautner, et al. 2018. “Immunization With a Recombinant Fusion Protein Protects Mice Against *Helicobacter pylori* Infection.” *Vaccine* 36: 5124–5132.
- Ghasemi, A., S. Wang, B. Sahay, J. R. Abbott, and R. Curtiss 3rd. 2022. “Protective Immunity Enhanced *Salmonella* Vaccine Vectors Delivering *Helicobacter pylori* Antigens Reduce *H. pylori* Stomach Colonization in Mice.” *Frontiers in Immunology* 13: 1034683.
- Ishigame, H., S. Kakuta, T. Nagai, et al. 2009. “Differential Roles of Interleukin-17A and -17F in Host Defense Against Mucoepithelial Bacterial Infection and Allergic Responses.” *Immunity* 30: 108–119.
- Jafarzadeh, A., T. Larussa, M. Nemati, and S. Jalapour. 2018. “T Cell Subsets Play an Important Role in the Determination of the Clinical Outcome of *Helicobacter pylori* Infection.” *Microbial Pathogenesis* 116: 227–236.
- Jang, S. C., S. R. Kim, Y. J. Yoon, et al. 2015. “In Vivo Kinetic Biodistribution of Nano-Sized Outer Membrane Vesicles Derived From Bacteria.” *Small* 11: 456–461.
- Jong, W. S., Z. Soprova, K. de Punder, et al. 2012. “A Structurally Informed Autotransporter Platform for Efficient Heterologous Protein Secretion and Display.” *Microbial cell factories* 11: 85.
- Kang, J. H., S. Park, J. Rho, et al. 2023. “IL-17A Promotes *Helicobacter pylori*-Induced Gastric Carcinogenesis via Interactions With IL-17RC.” *Gastric Cancer* 26: 82–94.
- Kaparakis-Liaskos, M., and R. L. Ferrero. 2015. “Immune Modulation by Bacterial Outer Membrane Vesicles.” *Nature Reviews Immunology* 15: 375–387.
- Keenan, J. I., R. A. Allardyce, and P. F. Bagshaw. 1997. “Dual Silver Staining to Characterise *Helicobacter* Spp. Outer Membrane Components.” *Journal of Immunological Methods* 209: 17–24.
- Kimoto, T., H. Kim, S. Sakai, E. Takahashi, and H. Kido. 2019. “Oral Vaccination With Influenza Hemagglutinin Combined With Human Pulmonary Surfactant-Mimicking Synthetic Adjuvant SF-10 Induces Efficient Local and Systemic Immunity Compared With Nasal and Subcutaneous Vaccination and Provides Protective Immunity in Mice.” *Vaccine* 37: 612–622.
- Li, B., Y. Xu, T. Xu, et al. 2022. “Disruption of sncRNA Improves the Protective Efficacy of Outer Membrane Vesicles Against *Helicobacter pylori* Infection in a Mouse Model.” *Infection and Immunity* 90: e0026722.
- Li, H., T. Liao, A. W. Debowski, et al. 2016. “Lipopolysaccharide Structure and Biosynthesis in *Helicobacter pylori*.” *Helicobacter* 21: 445–461.
- Li, X., Y. Liu, M. Wang, et al. 2024. “Safety, Pharmacokinetics, and Efficacy of Rifasutenizol, a Novel Dual-Targeted Antibacterial Agent in Healthy Participants and Patients in China With *Helicobacter pylori* Infection: Four Randomised Clinical Trials.” *Lancet Infectious Diseases* 24: 650–664.
- Liou, J. M., P. Malfertheiner, S. I. Smith, E. M. El-Omar, and M. S. Wu. 2024. “40 Years After the Discovery of *Helicobacter pylori*: Towards Elimination of *H. pylori* for Gastric Cancer Prevention.” *Lancet* 403: 2570–2572.
- Liu, K. Y., Y. Shi, P. Luo, et al. 2011. “Therapeutic Efficacy of Oral Immunization With Attenuated *Salmonella Typhimurium* Expressing *Helicobacter pylori* CagA, VacA and UreB Fusion Proteins in Mice Model.” *Vaccine* 29: 6679–6685.
- Liu, Q., X. Li, Y. Zhang, et al. 2019. “Orally-Administered Outer-Membrane Vesicles From *Helicobacter pylori* Reduce *H. pylori* Infection via Th2-biased Immune Responses in Mice.” *Pathogens and Disease* 77, no. 5: ftz050.
- Liu, Q., Q. Liu, J. Yi, et al. 2016. “Outer Membrane Vesicles From Flagellin-Deficient *Salmonella Enterica* serovar *Typhimurium* Induce Cross-Reactive Immunity and Provide Cross-Protection Against Heterologous *Salmonella* Challenge.” *Scientific Reports* 6: 34776.
- Liu, Q., K. Tan, J. Yuan, et al. 2018. “Flagellin-Deficient Outer Membrane Vesicles as Adjuvant Induce Cross-Protection of *Salmonella Typhimurium* Outer Membrane Proteins Against Infection by Heterologous *Salmonella* Serotypes.” *International Journal of Medical Microbiology* 308: 796–802.

- Maldonado, R. F., I. Sá-Correia, and M. A. Valvano. 2016. "Lipopolysaccharide Modification in Gram-Negative Bacteria During Chronic Infection." *FEMS Microbiology Review* 40: 480–493.
- Moran, A. P. 2008. "Relevance of Fucosylation and Lewis Antigen Expression in the Bacterial Gastrointestinal Pathogen *Helicobacter pylori*." *Carbohydrate Research* 343: 1952–1965.
- Nedrud, J. G., and T. G. Blanchard. 2001. "Helicobacter Animal Models." *Current Protocols in Immunology*. Chapter 19, Unit 19.8.
- Pardi, N., and F. Krammer. 2024. "mRNA Vaccines for Infectious Diseases—Advances, Challenges and Opportunities." *Nature Reviews Drug Discovery* 23: 838–861.
- Rubin, E. J., and M. S. Trent. 2013. "Colonize, Evade, Flourish: How Glyco-Conjugates Promote Virulence of *Helicobacter pylori*." *Gut Microbes* 4: 439–453.
- Rudnicka, W., E. Czkwianianc, I. Planeta-Malecka, et al. 2001. "A Potential Double Role of Anti-Lewis X Antibodies in *Helicobacter Pylori*-Associated Gastrointestinal Diseases." *FEMS Immunology and Medical Microbiology* 30: 121–125.
- Sabado, R. L., S. Balan, and N. Bhardwaj. 2017. "Dendritic Cell-Based Immunotherapy." *Cell Research* 27: 74–95.
- Schmidinger, B., K. Petri, C. Lettl, et al. 2022. "Helicobacter pylori Binds human Annexins via Lipopolysaccharide to Interfere With Toll-Like Receptor 4 Signaling." *Plos Pathogens* 18: e1010326.
- Seib, K. L., M. Scarselli, M. Comanducci, D. Toneatto, and V. Masignani. 2015. "Neisseria Meningitidis Factor H-Binding Protein fHbp: A Key Virulence Factor and Vaccine Antigen." *Expert Review of Vaccines* 14: 841–859.
- Singh, B., S. Jaiswal, and P. Kodgire. 2024. "Outer Membrane Proteins and Vesicles as Promising Vaccine Candidates Against *Vibrio* Spp. Infections." *Critical Reviews in Microbiology* 50: 417–433.
- Song, Z., B. Li, Y. Zhang, et al. 2020. "Outer Membrane Vesicles of *Helicobacter pylori* 7.13 as Adjuvants Promote Protective Efficacy Against *Helicobacter pylori* Infection." *Frontiers in Microbiology* 11: 1340.
- Srivastava, R., A. Kashyap, M. Kumar, G. Nath, and A. K. Jain. 2013. "Mucosal IgA & IL-1 β in *Helicobacter pylori* Infection." *Indian Journal of Clinical Biochemistry* 28: 19–23.
- Suresh, M. R., M. B. Fanta, J. Kriangkum, Q. Jiang, and D. E. Taylor. 2000. "Colonization and Immune Responses in Mice to *Helicobacter pylori* Expressing Different Lewis Antigens." *Journal of Pharmacy & Pharmaceutical Sciences [Computer File]* 3: 259–266.
- Tan, K., R. Li, X. Huang, and Q. Liu. 2018. "Outer Membrane Vesicles: Current Status and Future Direction of these Novel Vaccine Adjuvants." *Frontiers in Microbiology* 9: 783.
- Tang, X., P. Wang, Y. Shen, et al. 2023. "Lipopolysaccharide O-Antigen Profiles of *Helicobacter pylori* Strains From Southwest China." *BMC Microbiology* 23: 360.
- Théry, C., K. W. Witwer, E. Aikawa, et al. 2018. "Minimal Information for Studies of Extracellular Vesicles 2018 (MISEV2018): A Position Statement of the International Society for Extracellular Vesicles and Update of the MISEV2014 Guidelines." *Journal of Extracellular Vesicles* 7, no. 1: 1535750.
- Tran, A. X., J. D. Whittimore, P. B. Wyrick, S. C. McGrath, R. J. Cotter, and M. S. Trent. 2006. "The Lipid A 1-Phosphatase of *Helicobacter pylori* Is Required for Resistance to the Antimicrobial Peptide Polymyxin." *Journal of Bacteriology* 188: 4531–4541.
- Wang, L., Z. Li, C. Y. Tay, B. J. Marshall, and B. Gu. 2024. "Multi-centre, Cross-Sectional Surveillance of *Helicobacter pylori* Prevalence and Antibiotic Resistance to Clarithromycin and Levofloxacin in Urban China Using the String Test Coupled With Quantitative PCR." *The Lancet Microbe* 5: e512–e513.
- White, D. W., S. R. Elliott, E. Odean, L. T. Bemis, and A. D. Tischler. 2018. "Mycobacterium Tuberculosis Pst/SenX3-RegX3 Regulates Membrane Vesicle Production Independently of ESX-5 Activity." *MBio* 9, no. 3: e00778–e00818.
- Whitfield, C., and M. S. Trent. 2014. "Biosynthesis and Export of Bacterial Lipopolysaccharides." *Annual Review of Biochemistry* 83: 99–128.
- Xie, W., W. Zhao, Z. Zou, L. Kong, and L. Yang. 2021. "Oral Multivalent Epitope Vaccine, Based on UreB, HpaA, CAT, and LTB, for Prevention and Treatment of *Helicobacter pylori* Infection in C57BL /6 Mice." *Helicobacter* 26: e12807.
- Yunle, K., W. Tong, L. Jiyang, and W. Guojun. 2024. "Advances in *Helicobacter pylori* Vaccine Research: From Candidate Antigens to Adjuvants-A Review." *Helicobacter* 29: e13034.
- Zhang, H., Z. Liu, Y. Li, et al. 2024. "Adjuvants for *Helicobacter pylori* Vaccines: Outer Membrane Vesicles Provide an Alternative Strategy." *Virulence* 15: 2425773.
- Zhang, X., S. Sang, Q. Guan, H. Tao, Y. Wang, and C. Liu. 2022. "Oral Administration of a Shigella 2aT32-Based Vaccine Expressing UreB-HspA Fusion Antigen With and Without Parenteral rUreB-HspA Boost Confers Protection against *Helicobacter pylori* in Mice Model." *Frontiers in Immunology* 13: 894206.
- Zhong, Y., J. Chen, Y. Liu, et al. 2020. "Oral Immunization of BALB/c Mice With Recombinant *Helicobacter pylori* Antigens and Double Mutant Heat-Labile Toxin (dmLT) Induces Prophylactic Protective Immunity Against H. pylori Infection." *Microbial Pathogenesis* 145: 104229.
- Zou, X., J. Hu, M. Zhao, et al. 2022. "Chemical Synthesis of the Highly Sterically Hindered Core Undecasaccharide of *Helicobacter pylori* Lipopolysaccharide for Antigenicity Evaluation With Human Serum." *Journal of the American Chemical Society* 144: 14535–14547.

Supporting Information

Additional supporting information can be found online in the Supporting Information section.